

1 Generation of autogenic knickpoints in laboratory landscape
2 experiments evolving under constant forcing.

3

4 Léopold de Lavaissière¹, Stéphane Bonnet¹, Anne Guyez¹, and Philippe Davy²

5 ¹ GET, Université de Toulouse, CNRS, IRD, UPS(Toulouse), France,

6 ² Univ Rennes, CNRS, Géosciences Rennes - UMR 6118, 35000 Rennes, France,

7 Correspondance to Léopold de Lavaissière (leopold.delavaissiere@gmail.com)

8

9 ABSTRACT

10 The upward propagation of knickpoints in **river longitudinal** profiles of rivers is commonly
11 related to discrete changes in tectonics, climate or base-level. However, the recognition that some
12 knickpoints may form autogenically, independently of any external perturbation, may challenge
13 these interpretations. We investigate here the genesis and dynamics of such autogenic knickpoints
14 in laboratory experiments at the drainage basin scale, where landscape evolved in response to
15 constant rates of base-level fall and precipitation. Despite these constant forcings, we observe that
16 knickpoints regularly initiate in rivers at the catchments' outlet throughout experiments duration.
17 The **upstream propagation rate of knickpoint** does not decrease monotonically in relationship with
18 the decrease **of their** drainage area as predicted by stream-power based models, but **it first**
19 increases **until** the mid-part of catchments **before decreasing**. Their initiation **at the outlet**
20 coincides with **a fairly abrupt** river narrowing **entailing an increase in** their shear stress. Then,
21 **once knickpoints have propagated upward**, rivers widen **entailing** a decrease in shear stress and
22 incision rate, **making the river lower than** the base-level fall rate, **This creates** an unstable situation
23 **which drives** the formation of a new knickpoint. **The experiments suggest a new cyclic and**
24 **autogenic** model of **knickpoints** generation **controlled by river width dynamics regardless of any**
25 **variations of climate or tectonic rates. This questions an interpretation of landscape**

Supprimé: the

Supprimé: s

Supprimé: ir

Supprimé: in

Supprimé: with a peak retreat rate in

Supprimé: s

Supprimé: and

Supprimé: ing

Supprimé: ing leads to

Supprimé: below

Supprimé: once knickpoints have propagated upward, creating

Supprimé: that ends up with

Supprimé: We propose a

Supprimé: cyclic

Supprimé: of autogenic knickpoints

42 ~~records focusing only on climate and tectonic changes without considering autogenic processes.~~1

43 Introduction

44 Knickpoints are discrete zones of steepened bed gradient that are commonly observed in ~~river~~
45 ~~longitudinal~~ profiles. Although they occasionally occur due to changes in bedrock properties (e.g. Duval
46 et al., 2004), in many cases they are dynamical features that propagate upstream along ~~drainage networks~~
47 ~~(Whipple and Tucker, 1999; Kirby and Whipple, 2012; Whittaker and Boulton, 2012).~~ In this last case,
48 they are commonly considered as formed in response to variations in external forcing such as uplift rate,
49 sea level or climate (e.g. Crosby and Whipple 2006; Berlin and Anderson, 2007; Kirby and Whipple,
50 2012; Whittaker and Boulton, 2012; Mitchell and Yanites, 2019) which opens the possibility of using
51 ~~knickpoints in landscapes to identify such changes. Several studies pointed out however that some~~
52 ~~knickpoints could be autogenic that is to say internally-generated without any variation in boundary~~
53 ~~conditions (e.g. Hasbargen and Paola, 2000, 2003; Finnegan and Dietrich, 2011). Understanding how~~
54 ~~knickpoints can form autogenically is therefore crucial for retrieving changes in external forcing from~~
55 ~~their occurrence in landscapes. Most observations of autogenic knickpoints formation come from~~
56 ~~experimental modelling (see for example Paola et al., 2009) their initiation being attributed to~~
57 ~~amplification of local instabilities in flume (Scheingross et al., 2019) and drainage basin scale~~
58 ~~(Hasbargen and Paola, 2000) experiments. In these latter experiments for example, successive~~
59 ~~knickpoints initiated despite constant external forcing (base-level fall and precipitation) throughout the~~
60 ~~duration of the runs, even when landscapes were at steady-state on average. Internal processes may also~~
61 ~~complexify the propagation of knickpoints as shown in the flume experiments of Cantelli and Muto~~
62 ~~(2014) and Grimaud et al. (2016) where a single discrete event of base-level drop result in the~~
63 ~~propagation of multiple waves of knickpoints.~~

64
65 ~~In this work, we consider the generation and dynamics of autogenic knickpoints in laboratory-scale~~
66 ~~drainage basins experiments forced by constant rate of base-level fall and steady precipitation. Such~~
67 ~~landscape experiments have been used successfully to explore how tectonics and climate impact erosion~~
68 ~~processes and the evolution of topography under controlled conditions (e.g. Hasbargen and Paola, 2000;~~

Supprimé: It illustrates the need to consider autogenic processes in the generation of knickpoints and for deciphering variation of tectonic and climatic processes from landscape records.¶

Supprimé: in rivers

Supprimé: their

Supprimé: the

Supprimé: of landscapes

Supprimé: ; Yanites et al., 2013

Supprimé: -

Déplacé (insertion) [1]

Supprimé: Unlike the commonly accepted idea that knickpoints are symptomatic of changing external forcing (e.g. Crosby and Whipple 2006; Berlin and Anderson, 2007; Kirby and Whipple, 2012; Whittaker and Boulton, 2012; Mitchell and Yanites, 2019),

Supprimé: s

Supprimé: they

Supprimé: also

Supprimé: Their consideration should then be

Supprimé: analysis of knickpoints observed

Supprimé: Autogenic knickpoints

Supprimé: has been observed for example in experimental drainage basins forced by constant rate of base-level (BL) fall by Hasbargen and Paola (2000). In their experiments, successive knickpoints initiated despite constant forcing, even when landscapes were at steady-state. Internal processes may also complexify the propagation of knickpoints as shown in flume experiments by Cantelli and Muto (2014) and Grimaud et al. (2016) who observed that a single discrete event of BL drop may result in the propagation of multiple knickpoints

Supprimé: Other flume experiments show that some knickpoints may generate autogenically along a river profile from the amplification of local instabilities (Scheingross et al., 2019).

Déplacé (insertion) [2]

Supprimé: W

Supprimé: here

Supprimé: BL

106 [Bonnet and Crave, 2003; Lague et al., 2003; Turowski et al., 2006; Bonnet, 2009; Singh et al., 2015;](#)
 107 [Sweeney et al., 2015; Moussirou and Bonnet, 2018](#)). This approach allows for the observation of
 108 [complex dynamics that are sometimes difficult to simulate numerically and sheds new light on the way](#)
 109 [natural landforms may evolve. Landscape experiments capture the tree-like structure of drainage](#)
 110 [networks, the supply of eroded material from hillslopes, and especially their fluctuations, which is a](#)
 111 [natural complexity that is not reproduced in flume experiments, for example. The experiments presented](#)
 112 [here have been performed using a new setup specifically designed to investigate the evolution of a large,](#)
 113 [meter-long, single drainage basin under controlled forcing condition. In previous similar catchment-](#)
 114 [scale experiments \(Hasbargen and Paola, 2000, 2003; Bigi et al., 2006; Rohais et al., 2012\) the outlet](#)
 115 [location was pinned to a narrow motor-controlled gate used to simulate base-level fall and which also](#)
 116 [set the river width at the outlet. A specificity of our setup here is to use a large gate instead of a narrow](#)
 117 [one, allowing experimental rivers to freely evolved downstream, with no constraints on their width. We](#)
 118 [report here results from experiments where successive knickpoints initiate near the outlet autogenically](#)
 119 [and propagate within drainage basins. The experiments emphasize a new model of autogenic knickpoint](#)
 120 [initiation and propagation driven by downstream river width dynamics.](#)

124 2 Methods

125 [We present here results from 3 experiments, BL05, BL10 and BL15, performed with different rates of](#)
 126 [base level fall, of respectively 5, 10 and 15 mm.h⁻¹ \(Table 1\).](#) The facility is a box with dimensions 100
 127 x 55 cm filled with silica paste [\(Fig. 1; see also Fig. S1 in the Supplemental Material\)](#). At its front side,
 128 a sliding gate, 41 cm-wide, drops down at constant rate, acting as the [base level](#). [The initial surface](#)
 129 [consists on a plane with a counterslope of ~3°, opposite to the base level-side \(Fig. 1C\).](#) During a run,
 130 runoff-induced erosion occurs in response to steady [base level fall](#) and rainfall ([mean rainfall rate is of](#)
 131 [95 mm.h⁻¹ with a spatial coefficient of variation \(standard deviation/mean\) of 35%](#)). [The mean spatial](#)

Supprimé: We observe that

Supprimé: and

Supprimé: propose

Supprimé: autogenic

Supprimé: According to a stream-power based celerity model (SPCM), their upstream propagation rate is predicted to depend non-linearly on drainage area (a proxy for discharge; Crosby and Whipple 2006; Berlin and Anderson, 2007), implying a monotonous decrease of retreat rate as they propagate upstream. This property can be used for example to invert their present location for dating the external perturbation responsible for their formation (Crosby and Whipple 2006; Berlin and Anderson, 2007). A recent experimental study however pointed out a potential inadequacy of this model when the upstream decrease in discharge is counterbalanced by the adjustment of the river width, resulting in a constant knickpoint retreat rate (Baynes et al., 2018). Some other studies also pointed out some limitation of SPCM to predict the actual propagation of knickpoints when the role of sediment supply is not considered (Cook et al., 2013).¶

Déplacé vers le haut [1]: Unlike the commonly accepted idea that knickpoints are symptomatic of changing external forcing (e.g. Crosby and Whipple 2006; Berlin and Anderson, 2007; Kirby and Whipple, 2012; Whittaker and Boulton, 2012; Mitchell and Yanites, 2019), several studies pointed out that they could also be autogenic, that is to say internally-generated without any variation in boundary condition (e.g. Hasbargen and Paola, 2000, 2003; Finnegan and Dietrich, 2011). Their consideration should then be crucial for retrieving changes in external forcing from analysis of knickpoints observed in landscapes. Autogenic knickpoints has been observed for example in experimental drainage basins forced by constant rate of base-level (BL) fall by Hasbargen and Paola (2000). In their experiments, successive knickpoints initiated despite constant forcing, even when landscapes were at steady-state. Internal processes may also complexify the propagation of knickpoints as shown in flume experiments by Cantelli and Muto (2014) and Grimaud et al. (2016) who observed that a single discrete event of BL drop may result in the propagation of multiple knickpoints. Other flume experiments show that some knickpoints may generate autogenically along a river profile from the amplification of local instabilities (Scheingross et al., 2019).¶

Déplacé vers le haut [2]: We consider here the generation and dynamics of autogenic knickpoints in laboratory-scale drainage basins experiments forced by constant rate of BL fall and steady precipitation. We observe that successive knickpoints initiate near the outlet and propagate within

Supprimé: Landscape experiments have been used successfully to explore how tectonics and climate impact erosion processes and the evolution of topography under controlled conditions (e.g. Hasbargen and Paola, 2000; ... [1])

Déplacé vers le bas [3]: (Fig. 1; see also Fig. S1 in the Supplemental Material)

Supprimé: .

Déplacé (insertion) [3]

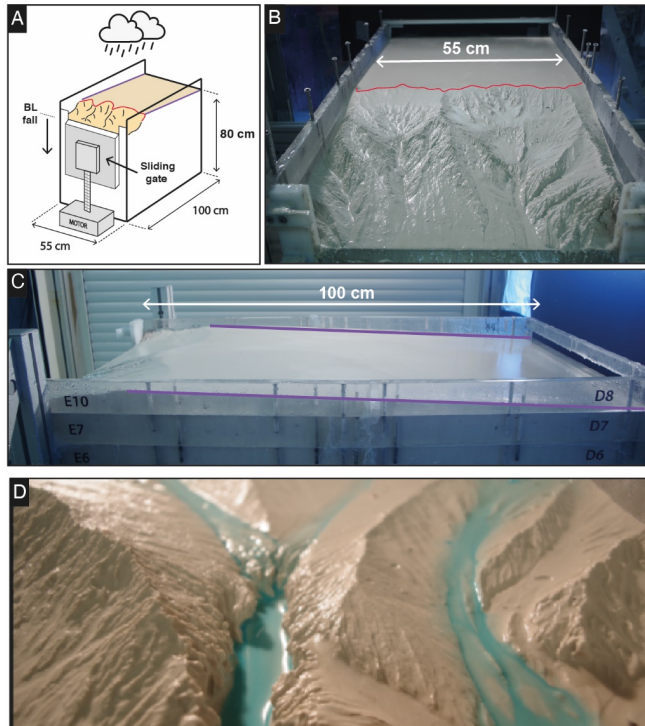
Supprimé: BL

Supprimé: artificial

Supprimé: and BL fall

211 precipitation rate of each experiment is of 95 mm.h^{-1} . Incisions initiate at some point along the base level
 212 and propagate upstream until a complete dissection of the initial surface. Note that the counterslope of
 213 the initial surface allows to separate the rainfall flux between the base level and the opposite side of the
 214 device and then to create a water divide (Fig. 1B).

Supprimé: Then, some
 Supprimé: i
 Supprimé: BL
 Supprimé: up to
 Supprimé: , which consists on a plane with a counterslope of $\sim 3^\circ$, opposite to the BL-side. This
 Supprimé: between incisions that develop along the BL-side and the initial surface. The use here of a large gate on the BL-side of the setup constitutes a major difference compared to previous similar catchment-scale experiments of Hasbargen and Paola (2000, 2003), Bigi et al. (2006) and Rohais et al. (2012). In these experiments, a single outlet location was actually pinned due a narrow gate, which also set the river width at the outlet. Unlike these experiments, the setup use here allows experimental rivers to freely evolved, with their width not being constrained by such a narrow gate.



215
 216 **Figure 1.** Experimental setup. Purple and red lines show respectively the counter-slope of the initial
 217 topography and the main water divide. (A) Sketch of the erosion box with the sliding gate, 41 cm wide,
 218 used to drop down the base level (BL). (B), (C) Front and side photographs (experiments BL10, at 525°
 219 and BL15 at 185°). (D) Photograph of a typical knickpoint studied here.

Supprimé: MBV07
 Supprimé: MBV06

221 **Table1. Parameters of experiments**

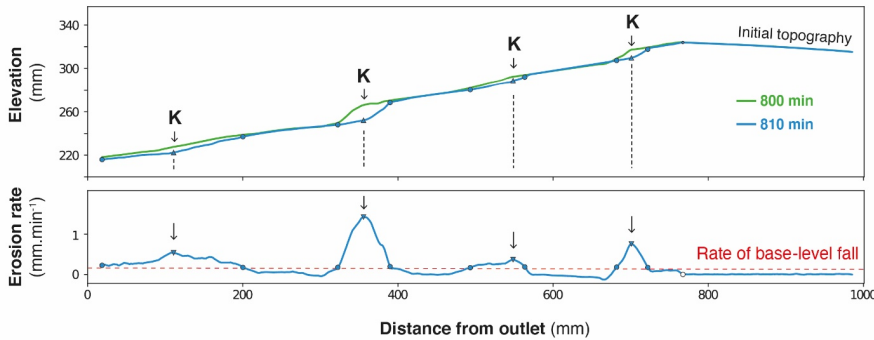
Experiments	Base Level Fall (mm/h)	Precipitation Rates (mm/h)	Duration Time (min)	Mean Divide Retreat Rates (mm/h)	nDDVmax	Mean Knickpoints Retreat Rates (mm/h)
BL15	15	95	1065	66.3	0.52	183.6 ± 93.8
BL10	10	95	1200	55.7	0.57	164.8 ± 74.8
BL05	5	95	1455	25	0.54	73.1 ± 50

240

241 Experiments were stopped every 5 min to digitize the topography using a laser sheet and to construct
 242 Digital Elevation Models (DEMs), with a pixel size of 1 mm. Longitudinal profiles and knickpoints were
 243 extracted with a semi-automatic procedure that had to be developed to process the ~200 DEMs per
 244 experiment. For this purpose, we first extracted longitudinal profiles by considering the lowest elevation
 245 on the successive rows of each DEM within a 20 cm-wide swath that included the main river and then
 246 by plotting it against distance down the long axis of the box. This procedure has already been applied
 247 by Baynes et al. (2018) and Tofelde et al. (2019). It may result in a slight overestimation in channel
 248 slope because it does not consider the obliquity of channels within the box in the distance calculation
 249 nor their sinuosity. However, these effects are of minor influence here, because most of channels are
 250 straight and roughly parallel to the long side of the box. In a second step, we computed the elevation
 251 difference between each successive pairs of longitudinal profiles and we identified knickpoints as peaks
 252 in erosion rates with values above the steady erosion amount defined by the rate of base-level fall (Fig.
 253 2). We verified manually that this procedure defines knickpoints correctly by checking the computed
 254 positions on longitudinal profiles. We investigated in particular if the procedure is robust with respect
 255 to the time interval between successive profiles. We found that the record interval of 5 minutes is too
 256 small to produce well-defined erosional peaks, which lead us to identify knickpoint positions from a
 257 time-interval of 10 minutes. Then, we built a first catalogue of knickpoints positions at different times,
 258 from which we manually extract the successive positions of each individual knickpoint. We
 259 complemented the database by computing incremental retreat rates of knickpoints from their successive
 260 positions.

261

- Supprimé: s
- Supprimé: Due to the large number of DEMs per experiment, about 200, river l
- Supprimé: based on
- Mis en forme : Police :(Par défaut) Times New Roman
- Mis en forme : Police :(Par défaut) Times New Roman
- Supprimé: in analysis of experiments
- Supprimé: , h
- Supprimé: most of channels being straight
- Supprimé: by considering
- Supprimé: carefully
- Supprimé: verified
- Supprimé: verified
- Supprimé: allows to
- Supprimé: and
- Supprimé: w
- Supprimé: how
- Supprimé: performed according
- Supprimé: chosen
- Supprimé: knickpoint retreats were generally
- Supprimé: when we considered the highest time-resolution of 5 minutes
- Supprimé: track
- Supprimé: at
- Supprimé: Thanks to this approach, we
- Supprimé: rough
- Supprimé: over
- Supprimé: that we subsequently rearranged manually by gathering together the
- Supprimé: then



290

291 **Figure 2.** Graph showing two successive longitudinal profiles of experiment *BL10* taken at 10 min
 292 interval (top) and corresponding erosion rate profile (bottom). Triangles illustrate the position of
 293 erosional peaks taken as knickpoint position (black arrows). Red dashed line shows the rate of base-
 294 level fall.

295

296 DEMs were also used to compute hydraulic information (water depth, river width, discharge and shear
 297 stress) using the Floodos hydrodynamic model of Davy et al. (2017; see also Baynes et al. (2018,
 298 2020) for previous use of Floodos for analyzing laboratory experiments). Floodos is a precipitation-based
 299 model that calculates the 2D shallow water equations (SWE) without inertia terms, from the routing of
 300 elementary water volumes on top of topography. We ran Floodos on successive DEMs of experiments
 301 by considering spatial distribution of precipitation, then generating several output raster products at the
 302 pixel size, including water depth, unit discharge and bed shear stress that were then used for
 303 computation of hydrologic parameters (river width, specific discharge and shear stress). The solution
 304 of the SWE depends on the friction coefficient (C) that depends on water viscosity only for laminar
 305 flow; its theoretical value is $\sim 2.5 \times 10^6 \text{ m}^{-1} \cdot \text{s}^{-1}$ at 10°C (Baynes et al., 2018). To ensure that Floodos
 306 outputs (e.g. water depth raster maps) calculated using this value are consistent with actual experiment
 307 hydraulic conditions, we injected dye in the rainfall water during a run to catch the actual extent of
 308 water flow and make rivers visible. A visual comparison with Floodos results shows a good match
 309 between model outputs and experimental results (Fig. S2), which validates the numerical method and

Supprimé: MBV07

Supprimé: ; see Supplemental Material

Supprimé: The output of floodos are maps of water depth, velocity and shear stresses.

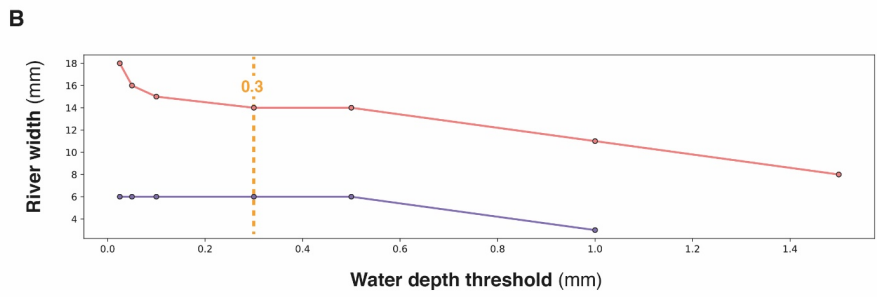
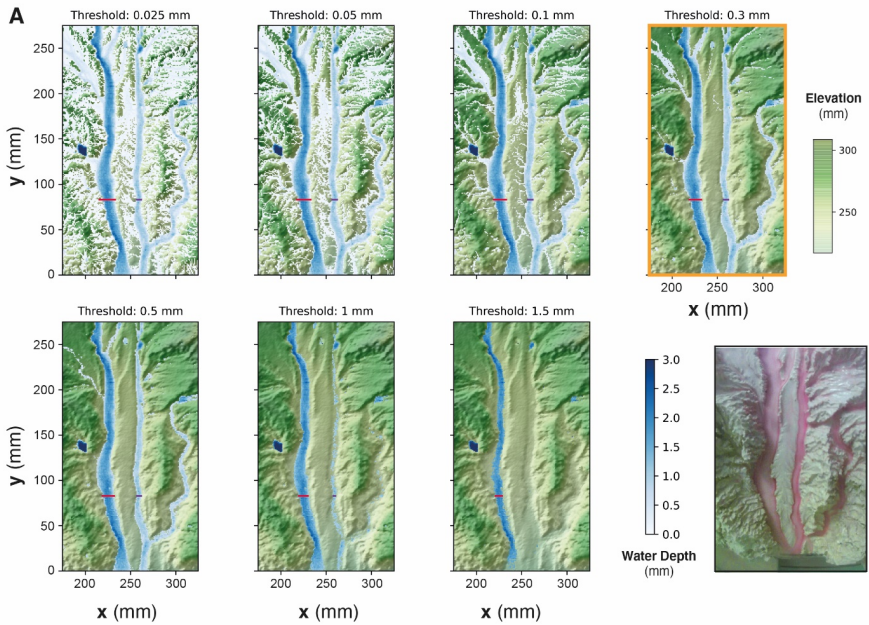
Mis en forme : Police :11 pt

Mis en forme : Police :(Par défaut) Times New Roman, 11 pt

Supprimé: (see Fig. 2 and Fig. S2)

315 the expected theoretical friction coefficient C (Baynes et al., 2018). Given the difficulty to measure the
 316 mm-scale water depth without perturbing the flow, river widths were extracted from Floodos DEM
 317 outputs by thresholding the water depth maps, river banks corresponding to sharp variations in water
 318 depth. The water depth threshold was estimated by trial and error by comparing the the rivers extracted
 319 from the calculation with direct observations on experiments where rainwater was colored by red dye
 320 (Fig. 3). A good visual agreement was obtained for a threshold value between 0.1 and 0.5 mm, and a
 321 mid-value of 0.3 mm was then used for determining river widths.

Supprimé: As,
 Supprimé: R
 Supprimé: considering
 Supprimé: and a threshold depth between channels and hillslopes. Floodos routing procedure calculates water depth from precipitation over the totality of the topography, on hillslopes as well as in channels,
 Supprimé: During runs, the actual water depth in rivers is very low, of mm-scale, and very difficult to measure without introducing any perturbation in the flow.
 Supprimé: hus, t
 Supprimé: varying this threshold over a DEM and by
 Supprimé: corresponding extent of rivers with actual extent of water flow as viewed
 Supprimé: injecting
 Supprimé: in the water used to produce the artificial rainfall
 Supprimé: consecutively



323

341 **Figure 3.** Impact of water depth threshold used to delineate river boundaries on estimated river widths,
342 considering a friction coefficient C of $2.5 \times 10^6 \text{ m}^{-1} \text{ s}^{-1}$. A. Map views of water depths (blue colors)
343 superimposed to DEM, for water depths threshold values between 0.025 and 1.5 mm. Red and purple
344 lines show corresponding river widths for two rivers. Photo on the bottom right shows the active river
345 width during the corresponding experimental run, viewed by injecting red dye in the water used to
346 generate the artificial rainfall. B. Corresponding local river widths for the two sections shown by red
347 and purple lines. The use of a low water depth threshold value (e.g. 0.025 mm; top left) leads to the
348 inclusion of large areas of shallow water depth in the “wetted area” considered as rivers and then to
349 unrealistic large rivers in comparison with actual rivers observed in the control run. On the opposite,
350 considering large threshold value (e.g. 1.5 mm) results in narrow rivers, or even in the absence of rivers
351 when maximum computed water depth is lower than this threshold. A threshold value of between 0.1
352 and 0.5 mm shows a good similarity between rivers on water depth map and the control run. Here, a
353 mid-value of 0.3 mm has been chosen for computing river widths.

Supprimé: (pink colors; “control run”)

Supprimé: thin

Supprimé: e

Supprimé: used

355 3 Results

356 3.1 Dynamics of knickpoints retreat

357 In each experiment, base level fall induces the growth of drainage networks by headward erosion and
358 the progressive migration of a main water divide (Fig. 4). The migration rate of the divide is constant in
359 each experiment (Fig. 5 and Table 1), and this value increases from 25 to 66 mm.h^{-1} with prescribed rate
360 of base level fall. The successive longitudinal profiles of the main river investigated in each experiment
361 (Fig. 6) illustrate the growth of rivers as they propagate within the box. These profiles show alternations
362 of segments with low and higher slopes, the later defining knickpoints. They regularly initiate at the
363 outlet throughout the duration of the runs in all experiments and propagate upward until they reach and
364 merge with the divide, some profiles showing even several knickpoints that retreat simultaneously (Fig.
365 6). A characteristic of these knickpoints highlighted in Figure 7 (see also Fig. 6) is that they generally
366 initiate downstream with a gentle slope and gradually steepen as they migrate upstream. Their maximum

Supprimé: We present here results from 3 experiments, MBV09, MBV07 and MBV06, performed with different rates of BL fall, of respectively 5, 10 and 15 mm.h^{-1} (Table 1).

Mis en forme : Justifié, Interligne : Double

Supprimé: BL

Supprimé: but

Supprimé: for increasing rate of

Supprimé: BL

378 slope is generally reached when they have propagated to the central part of the profiles (see below).
379 Then the slope is maintained or slightly decreases during their retreat in the upper segment of the
380 profiles.

381 ▼
382 The mean retreat velocity of knickpoints varies between experiments from 73 ± 50 to 183 ± 94 mm.h⁻¹

383 (Table 1) and increases as a function of the rate of base-level fall. Data suggest a non-linear relationship
384 between base-level fall rate and mean retreat velocity of knickpoints, however complementary

385 experiments would be necessary to constraint this dependency. To investigate the propagation of the
386 knickpoints, we built space-time diagrams (Fig. 8) by considering the successive alongstream position

387 of each knickpoint over experimental runtime, as well as the position of the water divide in the box as
388 already reported in Figure 5. To compare the dynamics of knickpoints within an experiment regardless

389 of the stage of water divide retreat into the box, the position of knickpoints (distance to outlet, D) has
390 been normalized to the position of the divide, hereafter referred to as normalized distance to divide

391 (nDD; nDD=0 at outlet and nDD=1 at the divide; Figure 4). Lines of isovalue of nDD considering an
392 increment of 0.1 are also shown in the space-time diagrams (Fig. 8). To a first order, the trajectories of

393 each knickpoint are very comparable within an experiment regardless the stage of retreat of the water
394 divide and the size of the catchment. Visually for example, in the space-time diagrams there is no

395 systematic variation in the general slope of the successive knickpoint trajectories over time, as the rivers
396 expand, that would indicate a change in mean knickpoint velocity in relation to the change in the river

397 length and catchment size. In detail, an inflection of trajectories is visible for many knickpoints when
398 they are close to the divide, for nDD > ~0.8 (Figure 8), which indicates that they slow down as they

399 approach the divide. The opposite is observed for some knickpoints when they are close to the outlet,
400 for nDD < ~0.2 / 0.3, with some trajectories suggesting, on the contrary, an acceleration after their

401 initiation (Figure 8; see also Fig. 7). These qualitative interpretations are supported by the detail analysis
402 of retreat velocity data shown in Figure 9. For each experiment, we show in Figure 9A the stack of

403 successive retreat velocities of each individual knickpoint according to distance nDD. The envelopes
404 draw a bell-shaped distribution for each experiment, which suggests, that retreat velocities are maximum

Supprimé: Figure 6 shows the evolution of the longitudinal profile of the main river investigated in each experiment, as well as topography of the initial surface, the profiles being colored according to the experimental runtime. These stacks illustrate the growth of rivers as they propagate within the box. Longitudinal profiles show alternations of segments with low and higher slopes, the later defining knickpoints that propagate upward, some profiles showing even several knickpoints that retreat simultaneously. Knickpoints regularly initiate at the outlet throughout the duration of the runs in all experiments, and propagate upward until they reach and merge with the divide.

Supprimé: in average

Supprimé: BL

Supprimé: show in Figure 7

Supprimé: In order to be able to

Supprimé: 2

Supprimé: in Figure 7

Supprimé: whatever

Supprimé: A

Supprimé: 7

Supprimé: 7

Supprimé: suppositions

Supprimé: 8

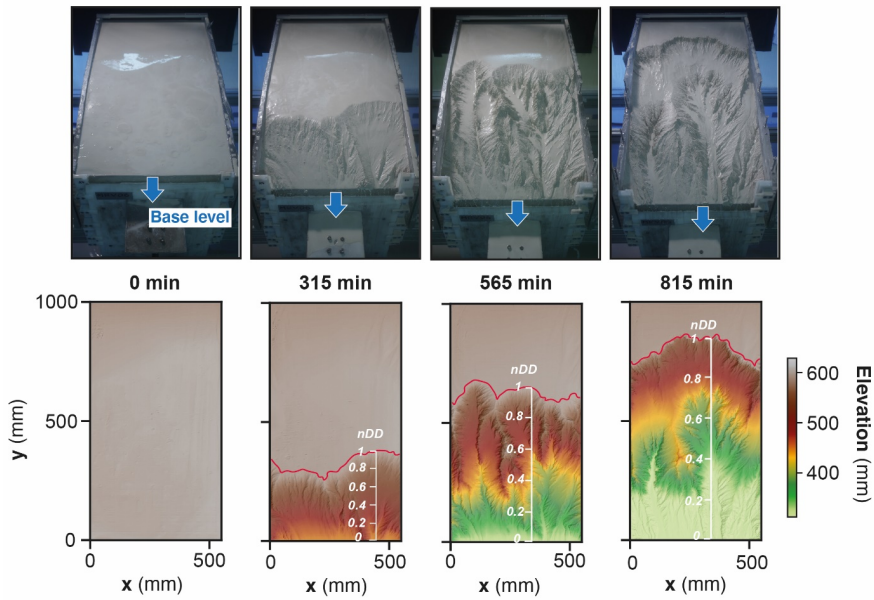
Supprimé: 8A

Supprimé: , i.e. according to their propagation between the outlet and the divide

Supprimé: indicates

433 when knickpoints are located at a mid-distance between the outlet and the divide, for central values of
 434 nDD, between 0.4 and 0.6. This is supported by summary statistics of retreat velocities at 0.1 intervals
 435 of nDD considering all knickpoints in each experiment (Fig. 9B). Both the mean and median values
 436 show higher rates of upstream propagation when knickpoints are in the central section of rivers in the
 437 three experiments, and conversely lower rates near the outlet ($nDD < 0.2 / 0.3$) where they initiate and
 438 start to propagate and near the divide ($nDD > 0.8$), as suggested by trajectories shown in Figure 8. Note
 439 that because knickpoint retreat rates also depend on the rate of base-level fall, the range of retreat rates
 440 is smaller in experiment with the lower rate of base level fall, BL05, so that their variation with distance
 441 is not as well defined as in both other experiments. However, the mean and median values are also
 442 slightly higher for intermediate distances which suggests that the trends described for the other two
 443 experiments are also valid here. Data from the three experiments indicate that after their initiation near
 444 the outlet, knickpoints first speed up with a maximum in the central part of the catchments before
 445 decelerating near the divide. It is worth noting that this specific trend of knickpoint retreat rates is
 446 observed regardless of the experiment stages and thus whatever the position of the divide, in the box.
 447 This applies both to rivers in the early stages of experiments evolution, i.e. when they are small as well
 448 as for very large rivers at the end of experiments. To further characterize this trend, we determined the
 449 position of maximum knickpoint velocity on longitudinal profiles, hereafter nDD_{vmax} , from a second
 450 order polynomial fit (Fig. 9C). This value is very similar between experiments, of 0.52, 0.57 and 0.54
 451 (Table 1).

- Supprimé: Figure 8b provides
- Supprimé: retreat
- Supprimé: n
- Supprimé: when they approach
- Supprimé: 7
- Supprimé: Then, these d
- Supprimé: accelerate
- Supprimé: and reach their maximum retreat rate
- Supprimé: to
- Supprimé: e
- Supprimé: as they approach
- Supprimé: distribution
- Supprimé: progress of the
- Supprimé: the advancement stage of incision and divide
- Supprimé: retreat
- Supprimé: to
- Supprimé: of experiments
- Supprimé: short
- Supprimé: , and to
- Supprimé: evolution of the
- Déplacé (insertion) [4]
- Supprimé: considered
- Supprimé: to the data shown in Figure 8 and used the inflexion to define a normalized longitudinal distance of maximum velocity of knickpoints
- Supprimé: 8
- Supprimé: referred to as nDD_{vmax} in the following
- Supprimé: 52 to 0.57

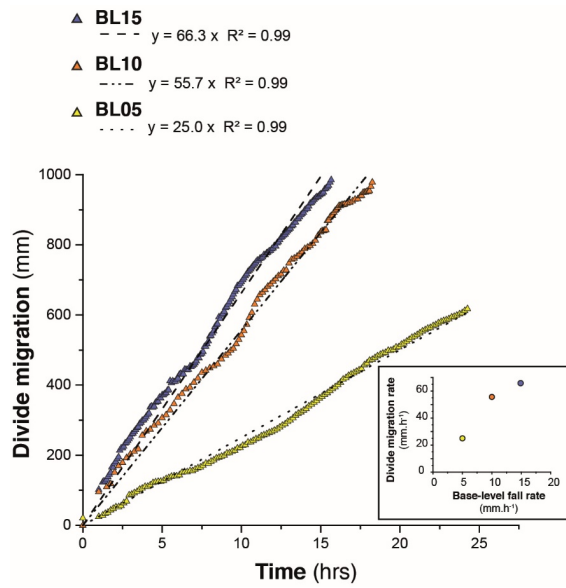


483

484 **Figure 4.** Photos and corresponding DEMs of experiment **BL15** at four runtimes. Note the propagation
 485 of the divide through the erosion box (red line) and the drop of the sliding gate used for falling base-
 486 level. The normalized distance to divide (nDD , see text) used to follow the position of knickpoints during
 487 runs is shown superimposed to DEMs.

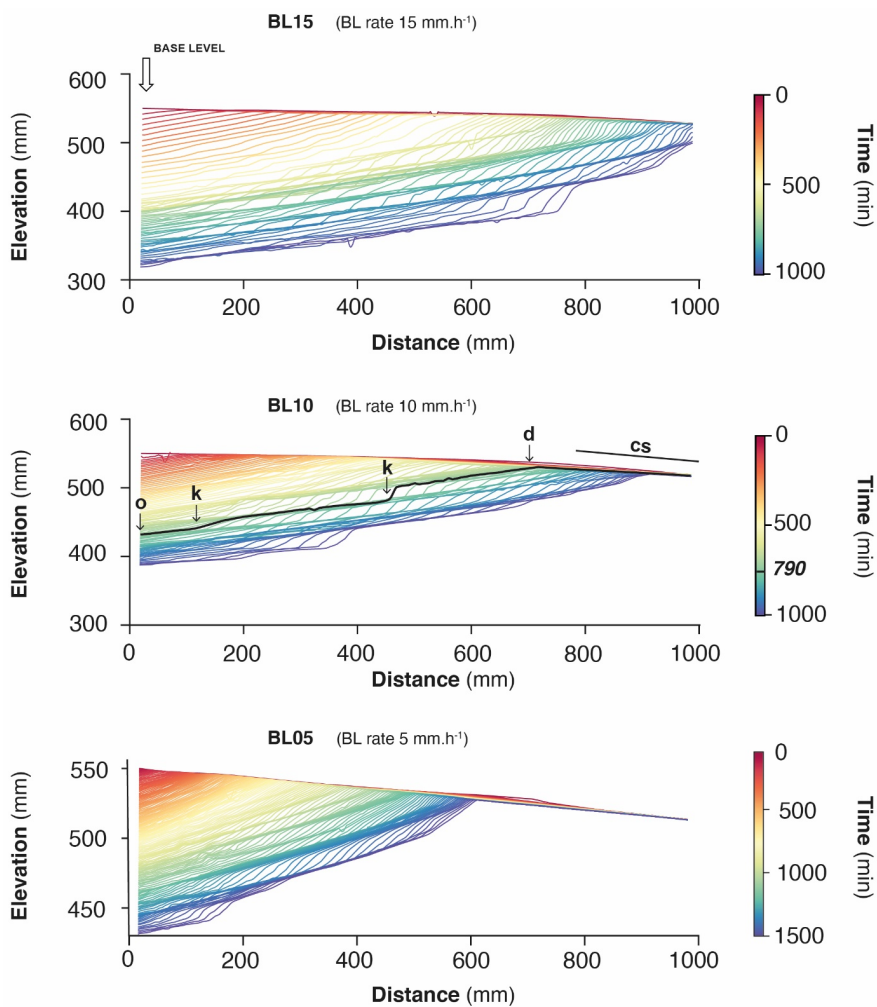
488

Supprimé: MBV06



490

491 **Figure 5.** Evolution of the water divide position within the erosion box for the three experiments. *The*
 492 *inset figure (Bottom right) show the relation between the divide migration rate in the three experiments*
 493 *and their related base-level fall rate.*

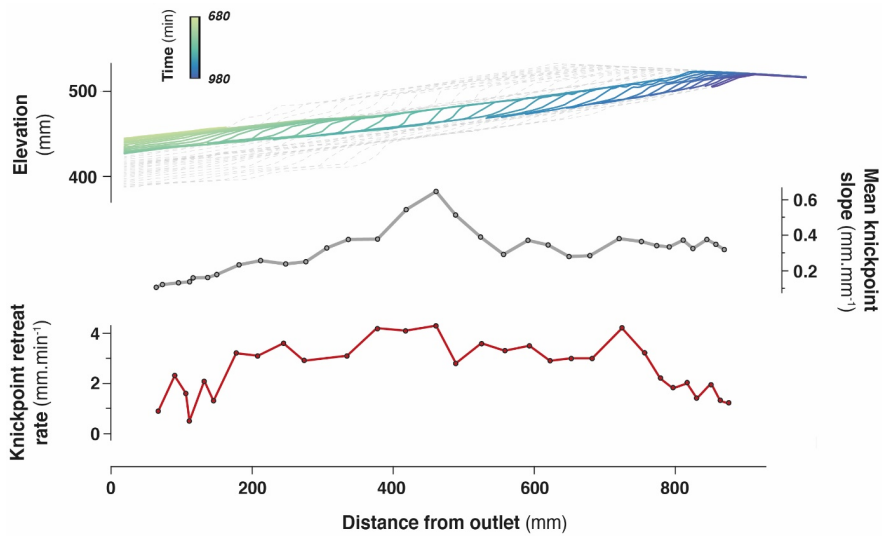


494

495 **Figure 6.** Successive river longitudinal profiles of experiments, shown here every 10 min. Each
 496 longitudinal profile is colored according to experimental runtime. The sliding gate used to drop the base
 497 level is to the left. Note the initial counterslope (cs). Black thick line on BL10 is the longitudinal profile
 498 at t=790', illustrating the outlet (o), knickpoints (k), and water divide (d). Note the change of scale for
 499 experiment BL05.

Supprimé: (BL)

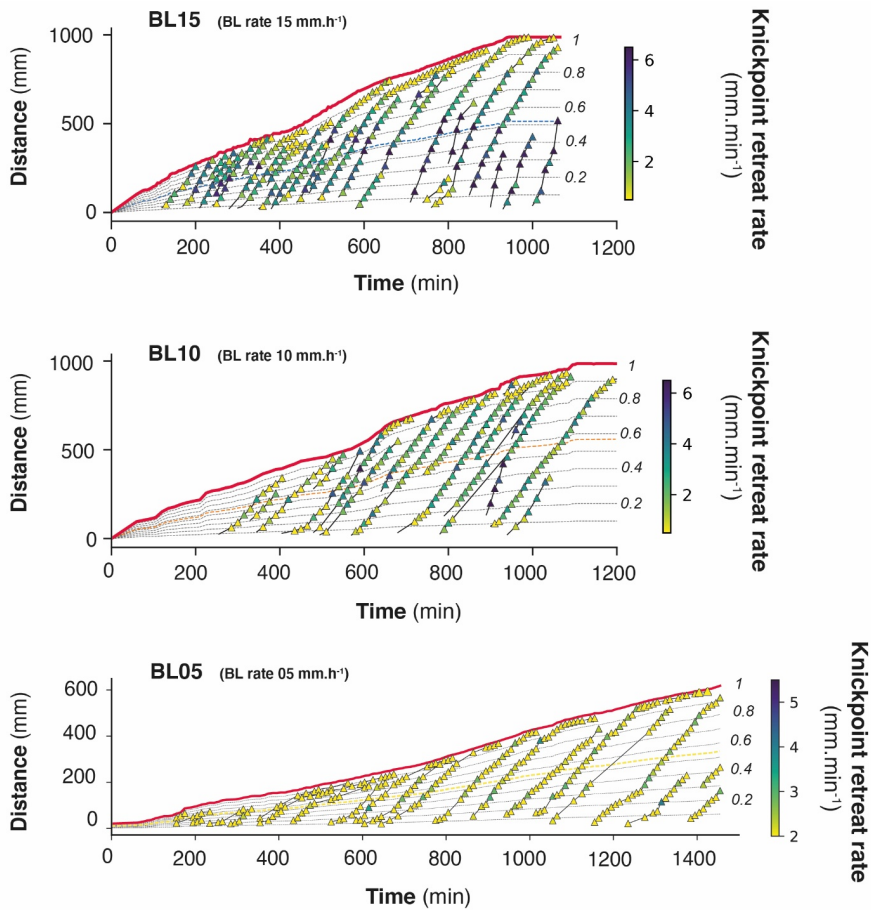
Supprimé: MBV07



502

503 **Figure 7.** Detail retreat of an individual knickpoint from experiment BL10 (see also Fig. 6) showing its
 504 initiation with a gentle slope which subsequently steepen as it migrates upstream (see also Fig. S3). Its
 505 maximum slope is reached at mid-distance between the outlet and the divide. Its lowest retreat rates are
 506 observed downstream near the outlet and upstream near the divide.

Supprimé: .



508

509

510 **Figure 8.** Space-time diagrams showing the propagation of the water divide (red line) and successive

511 trajectories of knickpoints (triangles). Symbols color shows instant (10 min) knickpoints retreat rate.

512 Thin **black** dashed lines show the normalized distances to divide (nDD). **Thin colored dashed lines show**

513 **nDD_{vmax}**, the normalized distance where the highest rate of retreat velocity is deduced from the analysis

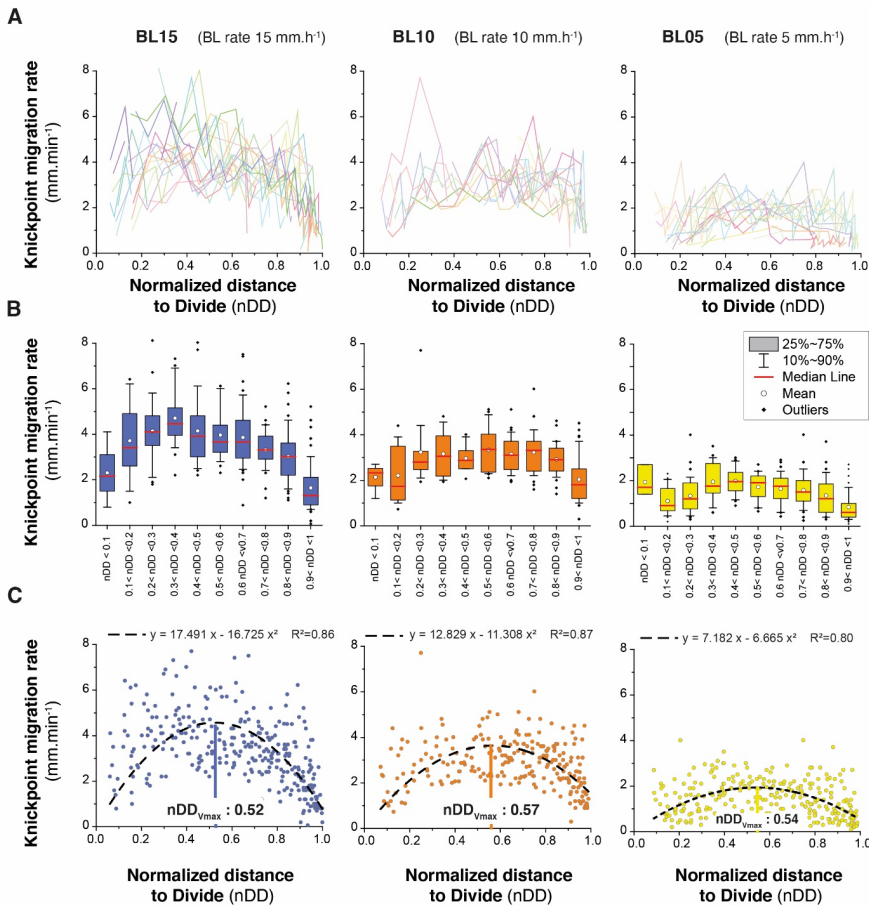
514 (see text and Figure 9C).

515

Supprimé: 7

Supprimé: distance where

Supprimé:



519

520 **Figure 9.** (A) Knickpoint retreat rates according to the normalized distances to divide (nDD) for each
 521 knickpoint of experiments. Each color line corresponds to an individual knickpoint of the space-time
 522 diagram in Fig. 8. (B) Summary statistics of retreat rates for nDD intervals of 0.1. (C) Plot of all
 523 knickpoints retreat rates for each experiment. Black dashed line shows the second order polynomial fit
 524 to the data used to define the normalized longitudinal distance of maximum velocity of knickpoints
 525 (nDD_{vmax}).

526

527

Supprimé : 8

Supprimé : 7

Mis en forme : Police :Gras

Déplacé vers le haut [4]: we considered a second order polynomial fit to the data shown in Figure 8 and used the inflexion to define a normalized longitudinal distance of maximum velocity of knickpoints (Fig. 8C) referred to as nDD_{vmax} in the following. This value is very similar between experiments, of 0.52 to 0.57 (Table 1).

Supprimé: Studies that investigated knickpoints retreat at catchment-scale demonstrated that their velocity decreases as they propagate upstream due to the progressive reduction of the upstream drainage area and water discharge (e.g. Crosby and Whipple, 2006. Berlin and Anderson, 2007). The pattern of velocity distribution that we document here is not consistent with this finding because we observe here an increase in knickpoints velocity in the early stage of their propagation. To evaluate this effect in our experiments, we investigated the dependency between retreat velocities and discharge by cutting the dataset into two parts corresponding to the different regimes identified above. For this purpose, we considered a second order polynomial fit to the data shown in Figure 8 and used the inflexion to define a normalized longitudinal distance of maximum velocity of knickpoints (Fig. 8C) referred to as nDD_{vmax} in the following. This value is very similar between experiments, of 0.52 to 0.57 (Table 1). Data above nDD_{vmax} (Figure 9) allows to consider retreat rates against more two orders of magnitude of unit discharge (total discharge normalized to river width). They do not show a clear tendency of increasing rate with discharge as expected, although a rough positive correlation could be defined, following a power law with an exponent of 0.25. Data below nDD_{vmax} show 3 distinct fields without any clear trend with discharge. The restricted range of discharge data however limits the analysis.

563

564

565

566 3.2 Knickpoints initiation

567 To illustrate how knickpoints initiated near the outlet, we consider here a 120 minutes-long sequence of
 568 channel evolution in experiment BL15 during which two knickpoints (K1 and K2) successively initiate
 569 and propagate upward (Fig. 10). In addition, we analyzed the history of channel width (Fig. 11A) and
 570 unit water discharge (Fig. 11B) at a cross-section located at 8 cm from the outlet (see location on Fig.
 571 10B). We also present a summary of the statistics of normalized elevation changes (Fig. 11C) and shear
 572 stress (Fig. 11D) for all pixels across the section. The sequence starts with a “standard” profile (i.e., a
 573 typical river profile without any perturbation) at runtimes 880 and 890 min once a previous knickpoint
 574 already propagated, still visible upstream in Figure 10A. The channel is 23 to 25 mm wide (Fig. 10B
 575 and 11A) and the unit discharge is about $1.5 \cdot 10^6 \text{ mm}^3 \cdot \text{h}^{-1} \cdot \text{mm}^{-1}$. Erosion in the channel is on average
 576 lower than the base level fall as normalized erosion is <1 for most pixels along the section (Fig. 11C).
 577 Then, the knickpoint K1 initiates at runtime 895' and starts to propagate upstream. At the surveyed
 578 section, the channel first narrows, up to ~15 mm wide at 905 min (~60 % decrease), and then widens
 579 (~25 mm) once the knickpoint has moved upstream of the section, at 910 min (Fig. 10B). The
 580 narrowing phase is naturally associated with an increase of the unit discharge (Fig. 11B) and with an
 581 enhanced erosion well above the base level fall rate, up to 4 times this rate in average at 900 min (Fig.
 582 11 C), with extremes as high as 8 times the base level rate. Once this knickpoint K1 has retreated, unit
 583 discharge decreases as the channel subsequently widens, to reach a width of 25 cm to 28 cm between
 584 925 and 930 min (Fig. 11A) while a new regular profile, i.e. without any slope break, established at 930
 585 min (Fig. 10A). The normalized erosion across the section decreases below the base level value (Fig.
 586 11C), with mean erosion rate values of 0.53, 0.36 and 0.76 times below the base level rates between 915
 587 to 925 min. Longitudinally, the profiles stack together downstream of the knickpoint following its retreat
 588 from 895 to 925 min (Fig. 10A), which also indicates minor vertical erosion here once the knickpoint

Supprimé: Figure 9. Relationship between knickpoints retreat rates and unit discharge (discharge/width) for $nDD < nDD_{Vmax}$ (left) and $nDD > nDD_{Vmax}$ (right).

Supprimé: MBV06

Supprimé: from experimental runtime 880 to 1000 minutes,

Supprimé: Figure 10 shows 5 min intervals sequence of downstream longitudinal profiles, 40 cm-long, showing their initiation and propagation as well as the evolution of a channel cross-section located at 8 cm from the box boundary

Supprimé: Some photos and perspective views of the corresponding DEMs also illustrate the evolution of the channel.

Mis en forme : Police : (Par défaut) Times New Roman

Supprimé: Complementary data are shown in Figure 11: variations over time of channel width (Fig. 11A) and unit water discharge (Fig. 11B) at the cross-section location as well as summary statistics of normalized elevation changes (Fig. 11C) and shear stress (Fig. 11D) for all pixels across the section. On the graph shown in Figure 11C, normalized values of 1 indicate erosion at the same rate than base-level fall and then steady-state conditions. Values > 1 or < 1 indicate respectively higher and lower erosion rate than BL fall rate. Negative values indicate sedimentation. The sequence starts with a regular profile at runtimes 880 and 890 min once a knickpoint has already retreated, still visible upstream (Figure 10A).

Supprimé: in

Supprimé: BL

Supprimé: B

Supprimé: the first

Supprimé: retreat

Supprimé: T

Supprimé: being

Supprimé: before to subsequently widenings

Supprimé:

Mis en forme : Police : (Par défaut) Times New Roman

Supprimé: retreated

Supprimé: at the location of the section surveyed

Supprimé: goes

Supprimé: in

Supprimé: BL

Supprimé: BL

Supprimé: first

Supprimé: decreased

Supprimé: BL

Supprimé: s

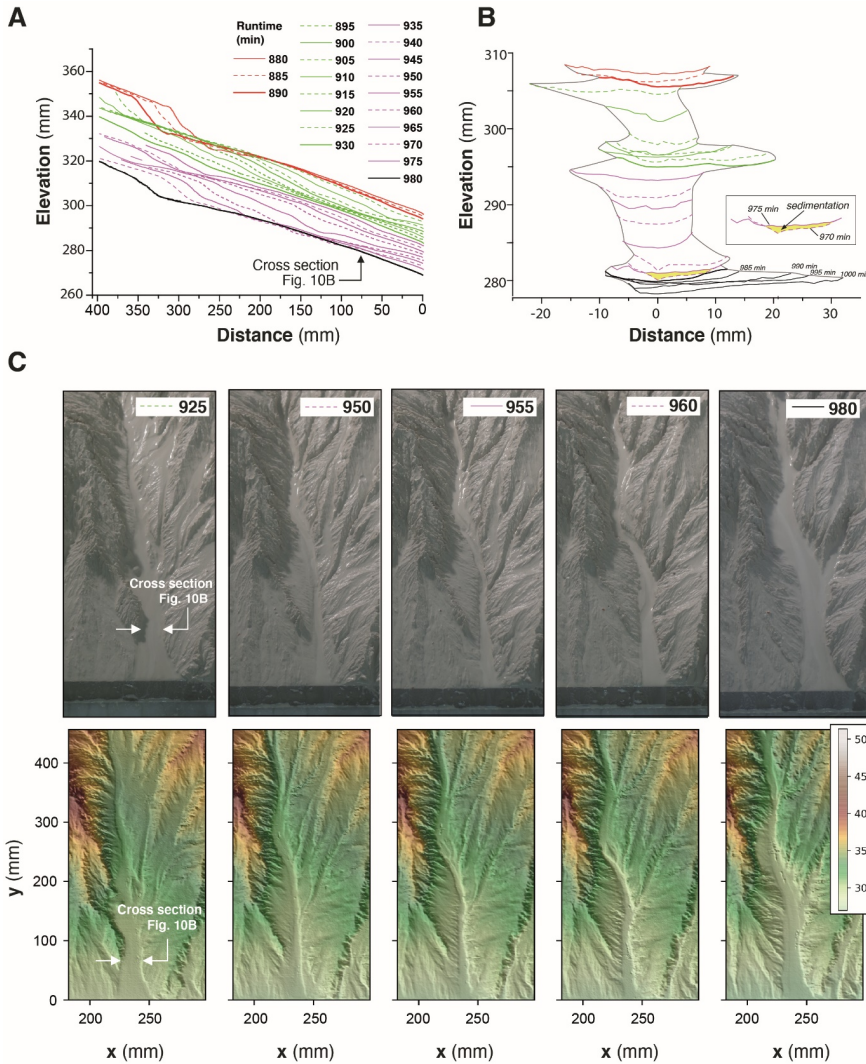
Supprimé: BL

634 has retreated despite the ongoing base level falling. The second knickpoint (K2) then initiates at 935
 635 min, propagates upstream in a similar way, and disappears leading to the setting up of a new regular
 636 profile at 980 min (Fig. 10A). Channel narrowing is also observed on the cross-section at the passage of
 637 this second knickpoint with a width that decreases to ~15 mm wide (Fig. 10B and 11A), associated with
 638 an increase of the unit discharge and the erosion rate (Fig. 11C). It is followed again by a phase of
 639 widening to reach a width to around 30 / 35 mm once the knickpoint has propagated upstream and by a
 640 decreasing erosion below the base level fall rate (Fig. 11C). Again, the longitudinal profiles stack
 641 together downstream of the knickpoint (Fig. 10A). Note that at 975 min, most of the surveyed section is
 642 undergoing sedimentation (mean normalized erosion rate is 0.1 and median is -0.25; Figures 10B and
 643 11C). The distribution of river bed shear stress along the section is given in the Figure 11D. Despite a
 644 large variability along the section, one can observe a significant increase of the median and maximum
 645 values at the time of the knickpoint passage, both for K1 and K2. Once knickpoints passed, the shear
 646 stresses decrease as the river widens.

647 This sequence illustrates that the rivers are never in equilibrium at the 5 min time-scale, but continuously
 648 oscillate over time between disequilibrium states with periods when channel are too wide to keep pace
 649 with the base level, and periods of knickpoint propagation when the erosion is enhanced to catch up the
 650 base level. The river width is the regulation parameter which allows the river erosion to adapt
 651 by increasing or decreasing the unit discharge. These knickpoints then propagate upward up to the divide
 652 as discussed previously (Fig. 6). The average erosion rate is similar to the baselevel fall rate (0.99) but
 653 it does not correspond to any stable configuration of the river since the erosion rate fluctuates between
 654 smaller and larger values. Knickpoints are by-products of this unsteady dynamics, which are generated

- Supprimé: falling
- Supprimé: A
- Supprimé: initiated
- Supprimé: and propagated
- Supprimé: until
- Supprimé: establishment
- Supprimé: The
- Supprimé: also coincides with a narrowing of the channel, being
- Supprimé: on the cross-section shown here
- Supprimé: a rise in the
- Supprimé: with an increase of the normalized erosion above the BL
- Supprimé: BL
- Déplacé (insertion) [5]
- Supprimé: sedimentation took place on a large part
- Supprimé:)
- Déplacé vers le haut [5]: Again, the longitudinal profiles stack together downstream the knickpoint (Fig. 10A).
- Supprimé: Figure 11D provides summary
- Supprimé: statistics of
- Supprimé: exerted on the channel bed
- Supprimé: for all pixels along the channel section.
- Supprimé: The values of shear stress show a quite
- Supprimé: large variability at the scale of the cross-
- Supprimé: with
- Supprimé: increasing however in phase with
- Supprimé: the passage of
- Supprimé: s
- Supprimé: Then o
- Supprimé: values
- Supprimé: periods of
- Mis en forme : Police : (Par défaut) Times New Roman
- Supprimé: during which erosion in wide channels goes at a slower rate than the BL and periods
- Supprimé: with
- Mis en forme : Police : (Par défaut) Times New Roman
- Supprimé: enhanced erosion and increased discharge in narrower rivers, erosion being well above the BL rate along the knickpoint segment

692 during the phases when the river catches up with its erosion deficit with respect to the base level.



693

694 **Figure 10.** Downstream knickpoints initiation and propagation in a 120 minutes-long sequence of
 695 experiment BL15 from experimental runtime 880 to 1000 minutes. (A) Sequence of downstream
 696 longitudinal profiles (5 min time-interval) of the investigated river, corresponding to the sequence
 697 hydro-geomorphic parameters shown in Figures 11 and 12. Propagation of the first (K1; initiated at

Supprimé: Although erosion appears to be fundamentally punctuated over time, considering all erosion rates data across the investigated cross-section and for the whole sequence shown here gives an average normalized erosion rate closed to unity (0.99) which indicates that these oscillations take place however around an average steady state over the long time-scale (erosion rate equal to BL rate). It indicates that enhanced erosion above the BL value during the retreat of knickpoint compensates the delay in vertical erosion that accumulates between two successive knickpoints, while rivers are defeated in following BL fall.

Supprimé:

Supprimé: Successive

Supprimé: downstream section

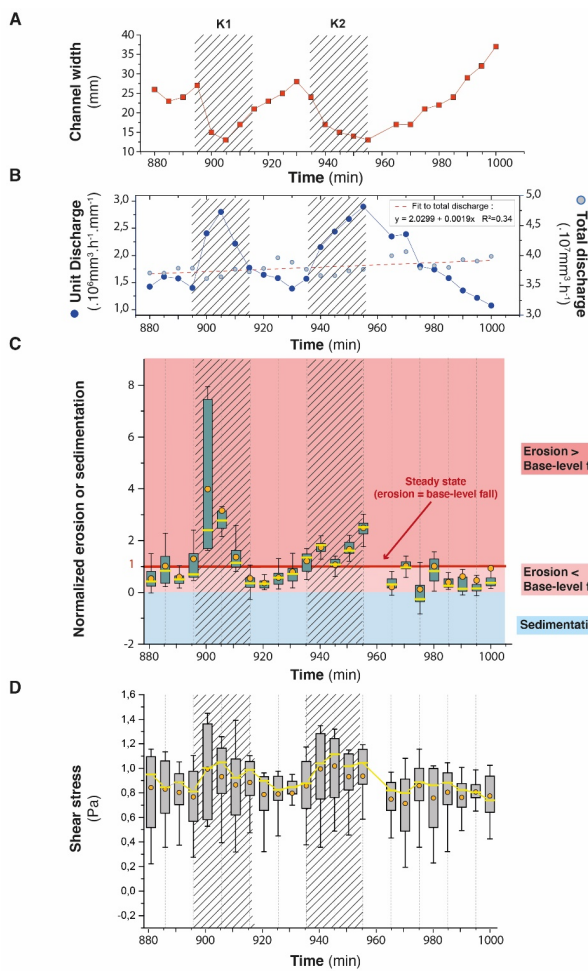
Supprimé: in experiment MBV06

713 895') and second (K2; initiated at 935') knickpoints is shown in green and purple colors respectively
 714 (see text). (B) Time evolution of successive cross-sections of the channel at 80 mm from the outlet. (C)
 715 Photos and perspective views of DEM at five time-steps.

Supprimé: is
 Supprimé: blue and orange

716

717



718

721 **Figure 11.** Time-series (5 min time interval) of river width (A) and unit and total discharge (B) for the
 722 channel in experiment BL15 shown in Figure 10B. Time-series of box-and-whisker plots of normalized
 723 erosion or sedimentation (C) and shear stress (D) for all pixels across the section. Orange solid circles
 724 and yellow lines show the mean and median values respectively. Edges of the boxes indicate the 25th
 725 and 75th percentiles. Note that in C, normalized values of 1 indicate erosion at the same rate than base-
 726 level fall and then steady-state conditions. Values > 1 or <1 indicate respectively higher and lower
 727 erosion rate than BL fall rate. Negative values indicate sedimentation. On all graphs, crosshatched
 728 areas indicate the passage of knickpoints K1 and K2.

729 To complement cross-section data, we also illustrate (Fig. 12) how parameters vary longitudinally by
 730 considering four stages, two before (925 min) and after (975 min) the passage of the knickpoint K2 and
 731 two during its retreat (945 and 950 min). Note that at 925 min, the previous knickpoint (K1) has just
 732 passed upstream the investigated profile and is responsible for the enhanced normalized erosion and
 733 increased shear stress upstream between distance 200 to 350 mm. Similarly, at 975 min the second
 734 knickpoint (K2) is still in the upstream part of the profile, between distance 300 to 350 mm. We also
 735 reported the longitudinal variations in river width, shear stress and normalized erosion along the profiles
 736 (Fig. 12). At runtimes 925 and 975 min, before and after the passage of knickpoint K2, erosion is below
 737 the base level rate along all the profiles down the knickpoints, with even localized sedimentation at 975
 738 min between 50 and ~150 mm. These sections are characterized by low shear stress values, being
 739 between 0.5 and 1 and by rivers that widen downward (around 0.7 mm/cm). On the opposite, during the
 740 passage of knickpoint K2, at runtimes 945 and 950 min, mean shear stress increases locally at the
 741 knickpoint location, being > 1 and the normalized erosion overpasses the base level rate there. These
 742 knickpoint segments are characterized by a narrowing of the rivers as already shown previously. The
 743 data illustrate that erosion mainly occurs during periods of knickpoint retreat though a combination of
 744 local steepening of the profile and narrowing of the river, resulting in an increased shear stress. On the
 745 opposite, once a knickpoint has propagated and between the passage of two successive knickpoints,
 746 erosion decreases significantly and does not longer compensate the base level fall. These periods of
 747 defeated erosion are characterized by low bed shear stress values in wide rivers, that widen downward.

Supprimé: at

Supprimé: MBV06

Supprimé: elevation

Supprimé: changes

Supprimé: F

Mis en forme : Police :Italique

Supprimé: C

Supprimé: show in Figure 12

Supprimé: second

Supprimé: first

Supprimé: 800

Supprimé: 650

Supprimé: ,

Supprimé: 700

Supprimé: 650

Supprimé: a

Supprimé: BL

Supprimé: 805

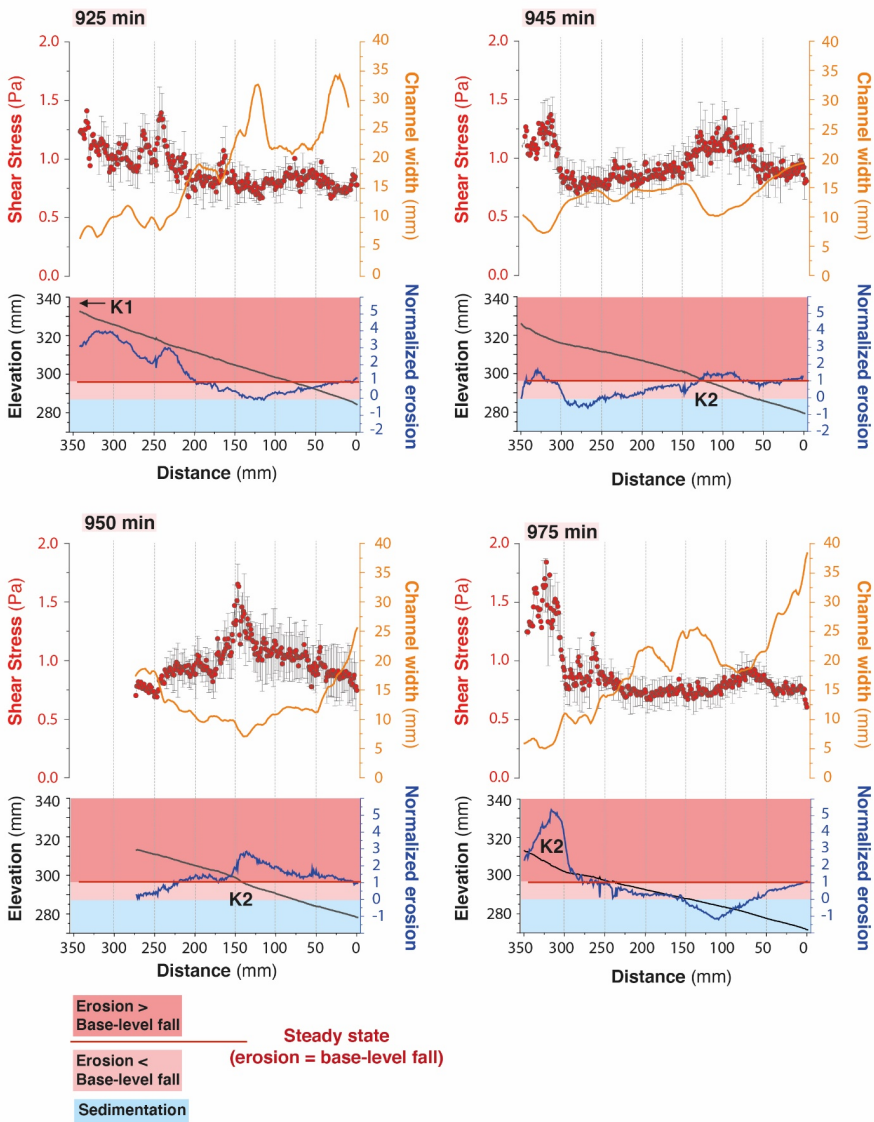
Supprimé: 950

Supprimé: a second

Supprimé: (K2)

Supprimé: BL

Supprimé: BL



770

771 **Figure 12.** Longitudinal trends of hydro-geomorphic parameters in experiment *BL15* at runtimes 925,
 772 945, 950 and 975 min (see text for comments). *K1* and *K2*: first and second knickpoints discussed in the
 773 text (see also Fig. 10A).

Supprimé: MBV 06

775

776 **4 Discussion**

777 **4.1 Autogenic knickpoints**

778 Our experiments illustrate the generation and retreat of successive knickpoint waves that traveled across
 779 the landscape during the growth of drainage networks. They formed throughout the duration of
 780 experiments regardless of the steadiness of the precipitation and **base level** fall rates and of the
 781 homogeneity of the eroded material. **These** knickpoints were autogenically generated (Hasbargen and
 782 Paola, 2000), arising only from internal geomorphic adjustments within the catchments rather than from
 783 variation in external forcing. Our observations appear very similar to those of Hasbargen and Paola
 784 (2000, 2003) and Bigi et al. (2006) who also reported the generation of successive **autogenic** knickpoints
 785 in landscape experiments evolving under steady forcing (rainfall and **base level** fall rate) throughout the
 786 duration of the runs. Unlike our experiments, which mainly consider the growth phase of drainage
 787 networks, experiments reported in Hasbargen and Paola (2000, 2003) and Bigi et al. (2006) considered
 788 the propagation of knickpoints after the phase of network growth, while their system was at steady-state
 789 on average (mean catchment erosion rate equals to **base level** rate). Then, given that the size of their
 790 experimental catchment was steady over time and given the steady rainfall rate, they were able to rule
 791 out variations of water discharge over time as **a** main driver for the generation of their knickpoints. On
 792 the opposite, in our experiments the size of catchments continuously increased over time, and thus the
 793 water discharge. However, this does not appear as **a** key factor controlling knickpoints initiation for
 794 several reasons. First, as we already mentioned, knickpoints arose at all stages of network growth and
 795 divide retreat, for both small and large rivers (Fig. 8), and thus whatever the range of water discharge at
 796 outlet. Second, the migration of the water divide related to drainage network growth occurred steadily
 797 and roughly at a constant rate during **the** experiments (see Figures 5 and 8), **as well as** the size of the
 798 catchments and the related increase in water discharge. Then, we can rule out abrupt variations in
 799 discharge as the driving mechanism for knickpoint initiation. Last, knickpoint initiations occurred at a
 800 higher frequency than the increase in water discharge that **resulted** from catchment expansion and divide
 801 migration. For example, in addition to unit discharge, we also reported on Figure 11B, the variation in

Supprimé: and conclusions

Supprimé: BL

Supprimé: Consequently, these

Supprimé: BL

Supprimé: ,

Supprimé: . These authors mentioned that their initiation was not "attributed to abrupt base-level drops, because the outlet drops continuously" (Hasbargen and Paola, 2000) as in our study

Supprimé: the

Supprimé: i

Supprimé: BL

Supprimé: the

Supprimé: the main

Supprimé: 7

Supprimé: an

Supprimé: 7

Supprimé: and then

Supprimé: results

Supprimé: C

822 total discharge during the 120 min-long sequence of knickpoint initiation discussed previously. The total
823 discharge rose from $3.7 \cdot 10^7$ to $4.0 \cdot 10^7$ $\text{mm}^3 \cdot \text{h}^{-1}$ in 120 minutes representing a $\sim 8\%$ increase, which is
824 relatively low compared to the $\sim 100\%$ increase of unit discharge during the passage of a knickpoint.
825 For all these reasons we conclude that the change in catchment size was not the main driver of successive
826 knickpoints initiation in our experiments, which occurred at a higher frequency.

Supprimé: occurs

827 4.2 Processes controlling knickpoints initiation and propagation

828 Given that the initiation of successive knickpoints was not related to changes in external factors and
829 catchment size over time, we consider internal geomorphic processes as driving mechanisms. The
830 detailed sequence of knickpoints initiation and propagation discussed above shows enhanced incision
831 above the rate of base level fall during the periods of knickpoints propagation. This occurred through
832 local steepening of the longitudinal profile and narrowing of the river, these two factors leading to an
833 increase in unit discharge and bed shear stress along the knickpoints. Several studies already
834 documented how steepening and narrowing act together for increasing river incision rate (e.g. Lavé and
835 Avouac, 2001; Duvall et al., 2004; Whittaker et al., 2007; Cook et al., 2013), which is what we also
836 document here. The novelty in our finding here, however, lies in the phase of post-knickpoint retreat.

Supprimé: Admitting

Supprimé: it is then necessary to

Supprimé: clearly

Supprimé: BL

Supprimé: section

837 Actually, immediately after the retreat of a knickpoint, we show that erosion is inhibited downstream
838 and rivers no longer incised despite the ongoing base level fall, until the passage of a new knickpoint.

Supprimé: BL

839 Although only illustrated in the sequence detailed previously (Figs. 10 to 12), this was a general behavior
840 that concerned the three experiments and their whole longitudinal profile, not only their downstream

Supprimé: clearly shown

Supprimé: presented here

841 part as in this sequence. Actually, this systematic decrease in erosion downstream of the knickpoints is
842 inherent to the geometry of the stacks of all successive longitudinal profiles of each experiment (Fig. 6).

Supprimé: e

Supprimé: discussed above

Supprimé: defeat

Supprimé: shown in

Supprimé: ure

843 In most cases, profiles downstream of retreating knickpoints stack on top of each other, as illustrated
844 schematically on Figure 13A, which indicates minor or no erosion downstream of the knickpoints until

Supprimé: BL

845 the passage of a new one. In the case of continuous adjustment of rivers to base level fall downstream
846 of the knickpoints, the geometry of profiles should rather show a pattern as illustrated in Figure 13B.

Supprimé: s

847 The pattern of profiles evolution over time documented here is usually observed following incremental
848 drops in base level (Finnegan, 2013; Grimaud et al., 2016) and to our best knowledge this is the first

Supprimé: a sudden and finite

Supprimé: BL

868 time here that such geometry is documented in the case of a continuous ~~base level~~ fall. This particular
869 pattern is explained by the decrease in erosion rate downstream ~~of~~ the retreating knickpoints which
870 finally acts as if the ~~base level~~ was not falling continuously at a constant rate but dropped regularly step-
871 by-step. Therefore, understanding the systematic occurrence of successive knickpoints in our
872 experiments requires to understand why erosion rate dropped downstream of knickpoints, following
873 their retreat. After the passage of knickpoints, we systematically observe a widening of the rivers, as
874 also documented in natural systems (e.g. Cook et al., 2014; Zavala-Ortiz et al., 2021) and a decrease in
875 the bed shear stress. Because an increase in channel width over time ~~inevitably reduces~~ the bed shear
876 stress if discharge and river gradient remain constant (Fuller et al., 2016), we propose that widening was
877 the main factor responsible for the decrease in shear stress and erosion rate after the passage of a
878 knickpoint, and then for the occurrence of the successive autogenic knickpoints. Demonstrating the sole
879 effect of river width on bed shear stress and erosion rate is complicated by covariations of these factors
880 with river slope and variations of discharge related to connection of tributaries. This can be ~~illustrated~~
881 however on the basis of the sequence ~~considered~~ previously, particularly at runtime 925 min between
882 the passage of ~~the~~ two successive knickpoints ~~K1 and K2~~ (Figs. 10 and 12). At that time, the profile of
883 the river ~~here~~ had a roughly constant slope (Fig. 14), without any slope break ~~and~~ no major tributary
884 connected (Fig. 10) that could ~~have significantly changed~~ the water discharge. As illustrated in Figure
885 12, this river segment was characterized by widening and decreasing shear stress downward ~~despite~~
886 ~~constant slope and total discharge~~. Then, ~~this example illustrates~~ a decrease in shear stress that was only
887 the result of the widening of the river downward (Fig. 14), ~~which~~ supports ~~the~~ hypothesis that defeated
888 erosion downstream ~~of~~ the propagating knickpoints was mainly due to the widening dynamics of the
889 experimental rivers.

Supprimé: BL

Supprimé: BL

Supprimé: will

Supprimé: discussed

Supprimé: discussed

Supprimé: (Fig. 14)

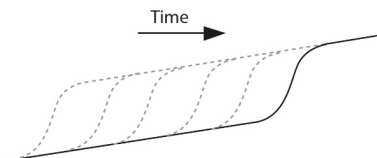
Supprimé: significantly

Supprimé: as shown in Figure 14 we can document here

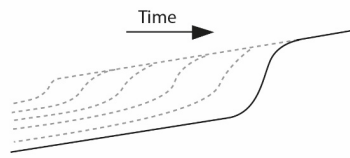
Supprimé: . This observation

Supprimé: our

A



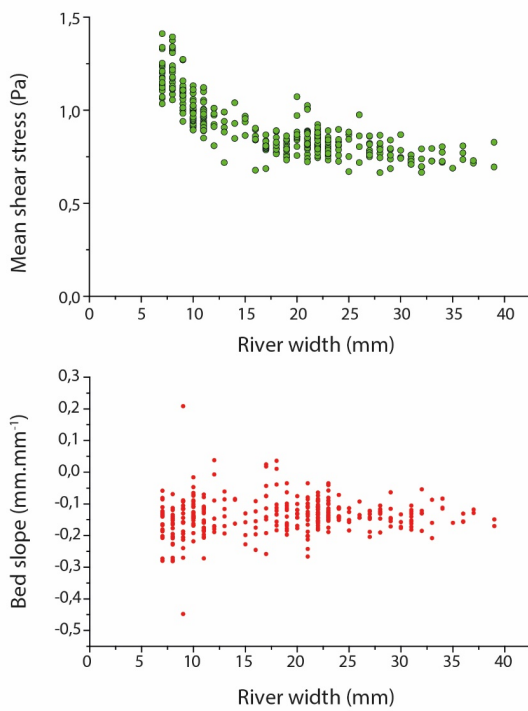
B



890

901 **Figure 13.** Sketches illustrating the difference in the geometry of successive longitudinal profiles
902 following the retreat of a knickpoint depending on whether fluvial incision is inhibited (A) or not (B)
903 downstream of the retreating knickpoint with respect to the continuously falling base level.

Supprimé: n



904

905 **Figure 14.** Top: river bed shear stress according to river width in the downstream section, 40 cm-long,
906 of experiment BL15 at runtime 925 (see also Fig. 12). Bottom: corresponding slope of the river bed.

Supprimé: MBV06

907 Incision of rivers in our experiments is fundamentally discontinuous despite continuous forcing and we
908 highlight downstream river width dynamics, in particular river widening, as a main cause of instability.
909 We show that once knickpoints have retreated, unit discharge, shear stress and incision rate all decrease
910 downstream while the rivers widen, resulting in a state where incision no longer counterbalance the
911 base-level fall. This results in an unstable situation that ends up with the initiation and propagation of a
912 new knickpoint and a new sequence of width narrowing, increasing shear stress and incision rate.

915 allowing the river to recover from the incision delay accumulated during the previous widening period.
916 Further work is required to understand the mechanisms responsible for lateral channel erosion in our
917 experiments, which is a key ingredient for understanding river mobility and widening. Several field (e.g.
918 Hartshorn et al., 2002; Turowski et al., 2008; Fuller et al., 2009), experimental (e.g. Wickert et al., 2013;
919 Bufe et al., 2016; Fuller et al., 2016; Baynes et al., 2020) and numerical (e.g. Turowski et al., 2007;
920 Lague, 2010; Langston and Tucker, 2018; Li et al., 2021) studies have demonstrated that high sediment
921 flux relative to transport capacity promotes increased lateral channel erosion. Most of these studies
922 highlight the role of cover effect, the protection of the river bed by transient deposition of sediments on
923 the river bed (Sklar and Dietrich, 2001; Turowski et al., 2007, 2008; Lague, 2010; Baynes et al., 2020;
924 Li et al., 2021), as a main factor promoting lateral erosion in high sediment flux settings. Other studies
925 show that by modifying the bed roughness, sediment deposition may deflect the flow, which also
926 promotes lateral erosion and widening (Finnegan et al., 2007; Fuller et al., 2016). Contrary to
927 experimental devices specifically designed to address these issues, large flumes in particular (e.g.
928 Finnegan et al., 2007; Fuller et al., 2016), direct observation on actual processes that drive lateral erosion
929 in our experiments is made difficult by the small size of the topographic features, the depth of rivers
930 being of millimeter scale, and by the low grain size of the material used. Opacity due to the generation
931 of the artificial rainfall also considerably limits direct observation during the runs. Despite these
932 limitations, data suggest that lateral erosion and river widening in our experiments is also related to
933 increase in sediment flux. We show actually that knickpoints are location of enhanced erosion well
934 above the rate of base level fall. We document for example mean erosion rates greater than 5 times the
935 base level fall rate, with extreme values up to a factor of 8 locally (Fig. 11 and 12). Downstream, where
936 rivers widen, we observe that the general decrease in erosion rate is also associated with local deposition
937 in some parts of the channels (for example at runtime 915 min in Figure 11 or 975 min in Figures 10 to
938 12). We then hypothesize that lateral erosion and widening are due in part to the increase sediment flux
939 related to enhanced erosion on knickpoints. Further work is needed to test this hypothesis, for example
940 by investigating in detail spatio-temporal variations in erosion and sedimentation during width
941 widening.

942 Further work is also needed to better understand how knickpoints initiate after the phases of widening,
943 in particular for determining whether river narrowing drives the formation of the knickpoints (e.g. Amos
944 and Burbank, 2007) or whether narrowing is a consequence of steepening (e.g. Finnegan et al., 2005).
945 Some studies that investigated the rivers response to increased uplift rate show that narrowing alone, at
946 constant river gradient, can allow rivers to increase their incision rate (Lavé and Avouac, 2001; Duvall
947 et al., 2004; Amos et al., 2007). In this context, Amos et al. (2007) propose a model in which the river
948 response to an increase in uplift rate first involves width narrowing, with the increase in slope and
949 formation of a knickpoint occurring only in a second stage, if the increase in incision induced by
950 narrowing is not sufficient to counteract the uplift rate. In our experiments here, we suggest that channel
951 narrowing predates, and in fact enables, the steepening of the profile in the initial stages of knickpoints
952 formation. Indeed, we observe that the transition from a wide to a narrow channel occurs very quickly,
953 at a smaller time scale than the time interval between two successive digitization of the experiments (5
954 min), and the knickpoints that form then have a very gentle slope, which then amplifies as they migrate
955 upstream (Fig. 7). This suggests that it is not the steepening that drives river narrowing but on the
956 contrary that narrowing is essential for knickpoints to initiate. Further work would also be needed to
957 verify this hypothesis, in particular with additional experiments with much higher frequency of data
958 acquisition to capture these changes in much more detail.

960 **4.3 Implications**

961 Knickpoints in river longitudinal profiles are commonly related to variations in tectonics or climate
962 through their influence on base level and/or sediment supply (e.g. Whipple and Tucker, 1999; Crosby
963 and Whipple, 2006; Kirby and Whipple, 2012; Whittaker and Boulton, 2012) and are then used to
964 highlight such changes when interpreting their occurrence in natural systems. The recognition here that
965 knickpoints may be generated autogenically due to cycles of river widening and narrowing is then of
966 first importance for retrieving information on tectonics and climate from their record in landscapes in
967 the form of knickpoints. Finding criteria that could be used in the analysis of natural systems to
968 differentiate these autocyclic knickpoints from those formed in response to tectonics or climate would

Supprimé: The set of experiments presented here illustrates the initiation and propagation of successive knickpoints during the growth of drainage networks and progressing enlargement of catchments, under constant external forcing. From the detailed analysis of their initiation and propagation, we propose that they formed autogenically, in response to variations in river width. We show that once knickpoints had retreated, unit discharge, shear stress and incision rate all decreased downstream while the rivers widened, resulting in a state where incision no longer counterbalanced the BL. fall. We propose that rivers widening downstream the retreating knickpoints is the main mechanism responsible for the decrease in incision rate through its feedback on unit discharge and shear stress. This results in an unstable situation that ends up with the initiation and propagation of a new knickpoint and a sequence of river narrowing, increasing shear stress and incision rate. Then, incision of rivers in these experiments appears to be fundamentally discontinuous despite continuous forcing, and we highlight downstream river width dynamics as the main driver. Unlike studies that documented how river narrowing leads to an increase in shear stress and incision rate (Lavé and Avouac, 2001; Duvall et al., 2004; Whittaker et al., 2007; Cook et al., 2013) we propose that the opposite, river widening, is potentially responsible for a decrease in erosion rate downstream a retreating knickpoint, leading ultimately to the generation of a new knickpoint. This specific mode of autogenic knickpoints initiation result in an upward dynamic of retreat that is not conventional, as we observe that they first accelerate during the first step of their propagation before to decelerate in a second time as they approach the divide. Actually,

1000 be an important step in the continuation of this work. A specificity of knickpoints in our experiments is
1001 to initiate downstream with a gentle slope, which then amplifies in the early stages of migration, and as
1002 a hypothesis we suggest that this may be characteristic of their autogenic formation following the
1003 mechanism described here. Being able to recognize these autogenic knickpoints would also be important
1004 for studies that investigate knickpoints propagation (e.g. Crosby and Whipple 2006; Berlin and
1005 Anderson, 2007; Schwanghart and Scherler, 2020) because knickpoints in our experiments are
1006 characterized by an upward dynamic of retreat that is not conventional. According to stream-power
1007 based celerity models, these studies consider that the upstream propagation rate of knickpoints depends
1008 inversely on drainage area (a proxy for discharge; Crosby and Whipple 2006; Berlin and Anderson,
1009 2007), implying a monotonous decrease of their retreat rate as they propagate upstream due to the
1010 progressive reduction of drainage area and water discharge. This property is used for example to invert
1011 their present location for dating the external perturbation responsible for their formation (Crosby and
1012 Whipple 2006; Berlin and Anderson, 2007). Here, knickpoints in our experiments first accelerate during
1013 their initial stages of propagation before, decelerating, in a second time as they approach the divide
1014 (Fig.9). Only this later phase of decreasing knickpoint velocity in the upstream part of rivers (for
1015 normalized distance $NDD > nDD_{v_{max}}$; Fig. 9) is consistent with predictions from stream-power based
1016 celerity models (see Fig. S3 in the Supplemental Material). On the opposite, a sole control by drainage
1017 area and discharge cannot explain the increase in velocity observed in the downstream sections (for
1018 $NDD < nDD_{v_{max}}$; Fig. 9), which implies an additional controlling factor. We suggest that this specific
1019 mode of retreat downstream is related to the progressive steepening of the knickpoints rather than to a
1020 purely hydrologic control. Deciphering the respective roles of slope and discharge in the retreat
1021 dynamics documented would require further in-depth analysis, particularly during the early stages of
1022 initiation and propagation which appear to be specific to the autogenic mechanism defined here.
1023 We show that the formation of knickpoints in our experiments is closely related to periods of decreasing
1024 erosion rate as the rivers widen, counterbalanced by increasing rate greater than the rate of base level
1025 fall as the rivers narrow and knickpoints form. Thus, the sequential evolution of longitudinal profiles is
1026 more consistent with the geometry that would be observed if the system was forced by discrete drop of

Supprimé: to

Supprimé: e

1029 the base level, rather than by a continuous base level drop as it is actually the case. We did not measure
1030 the sediment flux at the output of our models, but we can assume that it would be characterized by
1031 fluctuations controlled by the frequency of knickpoint initiation, superimposed on a longer-term
1032 increasing trend related to the growth of drainage networks. Some sediment outflux fluctuations were
1033 actually measured by Hasbargen and Paola (2000) in their experiments and interpreted as the
1034 consequence of knickpoint propagation. This study and our work illustrate that fluctuations in sediment
1035 flux can be observed at catchments outlet despite constant forcing parameters, when autocyclic
1036 knickpoints are generated in river systems.

1037 By performing such exploratory experiments, we do not pretend to reproduce natural landscapes in the
1038 laboratory because of important scaling issues (see Paola et al., 2009 for an extensive reflection on this
1039 matter) but rather to highlight and document complex system behaviors under controlled conditions that
1040 could provoke further investigations. Our findings support ongoing investigations that aim in better
1041 understanding the links between lateral erosion, channel geometry and valley width which is an issue
1042 that is emerging in the last years (e.g. Turowski, 2018; Croissant et al., 2019; Langston and Tucker,
1043 2019; Baynes et al., 2020; Zavala-Ortiz et al., 2021). A perspective to our work would be to investigate
1044 the mechanism of knickpoints generation driven by river width variations and the conditions that lead
1045 to their formation using landscape evolution models that incorporate lateral erosion and a dynamic river
1046 width (e.g. Davy et al., 2017; Carretier et al., 2018; Langston and Tucker, 2019). Simulations of
1047 Langston and Tucker (2019) highlight the role of bedrock erodibility as an important factor controlling
1048 lateral migration of rivers and the width of valleys, an issue that has not been investigated here given
1049 the similarity of the eroded materials in our experiments here. This study also confirms the assumption
1050 of Hancock and Anderson (2002) that lateral erosion and widening occurs preferentially in contexts of
1051 low incision rate, *i.e.* in domains with low uplift rate. This is likely in such contexts that the new mode
1052 of autogenic knickpoints formation driven by river width dynamics that we define in this study should
1053 apply.

1054 **5 Conclusions**

1055 Knickpoints in the longitudinal profile of rivers are commonly considered as incisional waves that
1056 propagate upstream through landscapes in response to changes in tectonics, climate or base-level. Based
1057 on results from a set of laboratory experiments at the drainage basin scale that simulate the growth of
1058 drainage networks in response to constant base level fall and rainfall, we show that knickpoints also
1059 form autogenically, independently of any variations in these external forcing factors. In all experiments,
1060 successive knickpoints initiate and propagate upward throughout the duration of the experimental runs,
1061 regardless of the rate of base level fall applied and of the size of the rivers as the catchments expand.
1062 Thanks to the computation of hydraulic information (water depth, river width, discharge and shear
1063 stress) using a hydrodynamic model, we show that the formation of knickpoints is driven by variations
1064 in river width at the outlet of catchments and we highlight width widening as a main cause of instability
1065 leading to knickpoint formation. Widening actually entails a decrease in shear stress and an incision rate
1066 lower than the rate of base level fall, resulting in an unstable situation that ends up with a sequence of
1067 width narrowing, increasing shear stress and incision rate as a knickpoint initiates. Rivers in our
1068 experiments thus evolve following sequences of width widening and narrowing that drive the initiation
1069 and propagation of successive knickpoints. As a result, incision is fundamentally discontinuous over
1070 time despite continuous forcing. It occurs during discrete events of knickpoint propagation that allows
1071 the rivers to recover from the incision delay accumulated during widening periods.

1072 ▼
1073 **Author contributions.** SB designed the experimental device. LdL, SB and AG built the experimental
1074 setup and carried out the experiments. LdL analyzed the data with the help of SB and PhD. All authors
1075 discussed the data. LdL and SB wrote the manuscript with input from AG and PhD.

1076
1077 **Acknowledgements.** This work was supported by ORANO-Malvesi and CNRS-INSU Tellus-Syster
1078 programme. We thank Sebastien Carretier and Odin Marc for fruitful discussions and Jens Turowski
1079 for his comments on a preliminary version of this manuscript. We thank Laure Guerit and an
1080 anonymous reviewer for their constructive comments which greatly improved the manuscript.▼

Supprimé: Based on results from a set of three laboratory experiments that simulate the growth of drainage networks in response to constant base level fall, we propose a new model of autogenic knickpoint formation driven by variations in river width at catchments' outlet. Obtaining these results was possible thanks to the development of a novel setup that allows the experimental rivers to freely evolved downstream near the base level, their width in particular not being constrained by the device. Knickpoints regularly initiate and propagate upward throughout the duration of the runs in all experiments and form autogenically, regardless of variation in external forcing and catchments size. Their initiation coincides with an increase in shear stress induced by river narrowing, leading to an increase in incision rate. Then, once knickpoints have propagated upward, rivers widen entailing a decrease in shear stress, and an incision rate lower than the rate of base level fall. This results in an unstable situation that ends up with the new phase of width narrowing and initiation of a new knickpoint. Thus, incision in our experiments occurs during discrete events of knickpoint propagation driven by river narrowing and **is then fundamentally discontinuous despite continuous forcing. We highlight downstream river width dynamics, in particular the decrease in erosion rate as rivers widen, as the main cause of instability.**¶
Contrary to predictions from stream-power based models, the upstream propagation rate of knickpoints formed in response to width variations does not decrease monotonically. Once initiated at outlet, they first speed up until the mid-part of catchments and then decelerate as they approach the divide. We relate this specific downstream trend of velocity to their initiation with a gentle slope as rivers narrow. ¶

Supprimé: This work was supported by ORANO-Malvesi. We thank Sebastien Carretier and Odin Marc for fruitful discussions and Jens Turowski for his comments on a preliminary version of this manuscript.

1116

1117 **References**

1118 [Amos, C.B., and Burbank, D.W.: Channel width response to differential uplift: *J. Geophys. Res.*, 112,](#)

1119 [doi:10.1029/2006JF000672, 2007.](#)

1120 Baynes, E.R.C., Lague, D., Attal, M., Gangloff, A., Kirstein, L.A., and Dugmore, A.J.: River self-
1121 organisation inhibits discharge control on waterfall migration: *Scientific Reports*, v. 8, p. 2444,
1122 doi:10.1038/s41598-018-20767-6, 2018.

1123 Baynes, E.R.C., Lague, D., Steer, P., Bonnet, S., and Illien, L.: Sediment flux-driven channel
1124 geometry adjustment of bedrock and mixed gravel–bedrock rivers: *Earth Surface Processes and*
1125 *Landforms*, v. 45, p. 3714–3731, doi:10.1002/esp.4996, 2020.

1126 Berlin, M.M., and Anderson, R.S.: Modeling of knickpoint retreat on the Roan Plateau, western
1127 Colorado: *Journal of Geophysical Research*, v. 112, p. F03S06, doi:10.1029/2006JF000553, 2007.

1128 Bigi, A., Hasbargen, L.E., Montarani, A., and Paola, C.: Knickpoints and hillslope failure: Interactions
1129 in a steady-state experimental landscape, *in* Willet, C.D., Hovius, N., Brandon, M.T., and Fisher,
1130 D.M., eds. *Tectonics, Climate and Landscape evolution*: Geological Society of America Special paper
1131 398, p. 295-307, doi:10.1130/2006.2398(18), 2006.

1132 Bonnet, S.: Shrinking and splitting of drainage basins in orogenic landscapes from the migration of the
1133 main drainage divide: *Nature Geoscience*, v. 2, p. 766–771, doi:10.1038/ngeo666, 2009.

1134 Bonnet, S., and Crave, A.: Landscape response to climate change: Insights from experimental
1135 modeling and implications for tectonic versus climatic uplift of topography: *Geology*, v. 31, p. 123–
1136 126, doi: 10.1130/0091–7613, 2003.

1137 [Bufe, A., Paola, C., and Burbank, D.W.: Fluvial beveling of topography controlled by lateral channel](#)
1138 [mobility and uplift rate: *Nature geosc.*, 9, 706-710, doi:10.1038/ngeo2773, 2016.](#)

1139 Cantelli, A., and Muto, T.: Multiple knickpoints in an alluvial river generated by a single drop in base
1140 level: experimental investigation: *Earth Surface Dynamics*, 2, 271-278, doi:10.5194/esurf-2-271-2014,
1141 2014.

1142 [Carretier, S., Godderis, Y., Maertinez, J., Reich, M., and Martinod, J.: Colluvial deposits as a possible](#)
1143 [weathering reservoir in uplifting mountains: *Earth Surf. Dynam.*, 6, 217-237, doi: 10.5194/esurf-6-](#)
1144 [217-2018, 2018.](#)

1145 Cook, K.L., Turowski, J.M., and Hovius, N.: A demonstration of the importance of bedload transport
1146 for fluvial bedrock erosion and knickpoint propagation: *Earth Surface Processes and Landforms*, v. 38,
1147 p. 683–695, doi:10.1002/esp.3313, 2013.

1148 Cook, K.L., Turowski, J.M., and Hovius, N.: River gorge eradication by downstream sweep erosion:
1149 *Nature geoscience*, doi:10.1038/NGEO2224, 2014.

1150 Croissant, T., Lague, D., and Davy, P.: Channel widening downstream of valley gorges influenced by
1151 flood frequency and floodplain roughness: *Journal of Geophysical Research-Earth Surface*, v. 124, p.
1152 154–174, doi:10.1029/2018JF004767, 2019.

1153 Crosby, B.T., and Whipple, K.X.: Knickpoint initiation and distribution within fluvial networks: 236
1154 waterfalls in the Waipaoa River, North Island, New Zealand: *Geomorphology*, v. 82, p. 16–38,
1155 doi:10.1016/j.geomorph.2005.08.023, 2006.

1156 ~~Davy, P., Croissant, T., and Lague, D.: A precipitation method to calculate river hydrodynamics, with~~
1157 ~~applications to flood prediction, landscape evolution models, and braiding instabilities: *Journal of*~~
1158 ~~*Geophysical Research-Earth Surface*, v. 122, p. 1491–1512, doi:10.1002/2016JF004156, 2017.~~

1159 Duvall, A., Kirby, E., and Burbank, D.: Tectonic and lithologic controls on bedrock channel profiles
1160 and processes in coastal California: *Journal of Geophysical Research*, v. 109, p. F03002,
1161 doi:10.1029/2003JF000086, 2004.

Supprimé: Davy, P., Croissant, T., and Lague, D.: A precipitation method to calculate river hydrodynamics, with applications to flood prediction, landscape evolution models, and braiding instabilities: *J. Geophys. Res.-Earth*, 122, 1491-1512, doi:10.1002/2016JF004156, 2017. [↗](#)

Mis en forme : Anglais (E.U.)

Mis en forme : Anglais (E.U.)

1167 Finnegan, N.J.: Interpretation and downstream correlation of bedrock river terrace trends created by
1168 propagation knickpoints: *Journal of Geophysical Research-Earth Surface*, v. 118,
1169 doi:10.1029/2012JF002534, 2013.

1170 [Finnegan, Noah J., Leonard S. Sklar, and Theodore K. Fuller. Interplay of sediment supply, river](#)
1171 [incision, and channel morphology revealed by the transient evolution of an experimental bedrock](#)
1172 [channel. *Journal of Geophysical Research: Earth Surface* 112.F3, doi:10.1029/2006JF000569, 2007.](#)

1173 [Finnegan, N.J., Roe, G., Montgomery, D.R., and Hallet, B.: Controls on the channel width of rivers:](#)
1174 [Implications for modeling fluvial incision of bedrock: *Geology*, 33, 229-232, doi:10.1130/G21171.1,](#)
1175 [2005.](#)

1176 [Fuller, T.K., Perg, L.A., Willenbring, J.K., and Lepper, K.: Field evidence of climate-driven changes](#)
1177 [in sediment supply leading to strath terrace formation: *Geology*, 37, 467-470,](#)
1178 [doi:10.1130/G25487A.1, 2009.](#)

1179 Fuller, T.K., Gran, K.B., Sklar, L.S., and Paola, C.: Lateral erosion in an experimental bedrock
1180 channel: The influence of bed roughness on erosion by bed load impacts: *Journal of Geophysical*
1181 *Research-Earth Surface*, v. 121, p. 1084-1105, doi:10.1002/2015JF003728, 2016.

1182 Grimaud, J.-L., Paola, C., and Voller, V.: Experimental migration of knickpoints: influence of style of
1183 base-level fall and bed lithology: *Earth Surface Dynamics*, v. 4, p. 11–23, doi:10.5194/esurf-4-11-
1184 2016, 2016.

1185 Hancock, G.S., and Anderson, R.S.: Numerical modeling of fluvial strath-terrace formation in
1186 response to oscillating climate: *Geological Society of America Bulletin*, v. 114, p. 1131-1142, 2002.

1187 [Hartshorn, K., Hovius, N., Dade, W.B., and Slingerland, R.L.: Climate-driven bedrock incision in an](#)
1188 [active mountain belt: *Science*, 297, 2036-2038, 2002.](#)

1189 Hasbargen, L.E., and Paola, C.: Landscape instability in an experimental drainage basin: *Geology*, v.
1190 24, p. 1067-1070, 2000.

Supprimé: Finnegan, N.J., and Dietrich, W.E.: Episodic bedrock strath terrace formation due to meander migration and cutoff: *Geology*, 39, 143-146, doi:10.1130/G31716.1, 2011.

1195 Hasbargen, L.E., and Paola, C.: How predictable is local erosion rate in erosional landscape ? *in*
1196 Wilcox, P.R. and Iverson, R.M., eds., Prediction in Geomorphology: American Geophysical Union
1197 Geophysical Monograph 135, doi:10.1029/135GM16, 2003.

1198 [Kirby, E., and Whipple, K.X.: Expression of active tectonics in erosional landscapes: Journal of](#)
1199 [Structural Geology](#), v. 44, p. 54–75, doi:10.1016/j.jsg.2012.07.009, 2012.

1200 [Lague, D.: Reduction of long-term bedrock incision efficiency by short-term alluvial cover](#)
1201 [intermittency: J. Geophys. Res., 115, doi:10.1029/2008JF001210, 2010.](#)

1202 [Lague, D., Crave, A., and Davy, P.: Laboratory experiments simulating the geomorphic response to](#)
1203 [tectonic uplift: Journal of Geophysical Research-Solid Earth](#), v. 108, doi:10.1029/2002JB001785,
1204 2003.

1205 [Langston, A.L., and Tucker, G.E.: Developing and exploring a theory for the lateral erosion of](#)
1206 [bedrock channels for use in landscape evolution models: Earth Surf. Dynam., 6, 1-27,](#)
1207 [doi:10.5194/esurf-6-1-2018, 2018.](#)

1208 Lavé, J., and Avouac, J.P.: Fluvial incision and tectonic uplift across the Himalayas of central Nepal:
1209 [Journal of Geophysical Research-Solid Earth](#), v. 106, p. 26561–26591, doi:10.1029/2001JB000359,
1210 2001.

1211 [Li, T., Venditti, J.G., and Sklar, L.S.: An analytical model for lateral erosion from saltating bedload](#)
1212 [particle impacts: J. Geophys. Res.– Earth, 126, doi:10.1029/2020JF006061, 2021.](#)

1213 Mitchell, N.A., and Yanites, B.J.: Spatially variable increase in rock uplift in the Northern U.S.
1214 Cordillera recorded in the distribution of river knickpoint and incision depths: [Journal of Geophysical](#)
1215 [Research: Earth Surface](#), v. 124, 1238-1260, doi:10.1029/2018JF004880, 2019.

1216 Moussirou, B., and Bonnet, S.: Modulation of the erosion rate of an uplifting landscape by long-term
1217 climate change: An experimental investigation: [Geomorphology](#), v. 303, p. 456–466,
1218 doi:10.1016/j.geomorph.2017.12.010, 2018.

Supprimé: Hilley, G.E., and Arrowsmith, J.R.: Geomorphic response to uplift along the Dragon's Back pressure ridge, Carrizo Plain, California: [Geology](#), v. 36, p. 367-370, doi:10.1130/G24517A.1, 2008.

Supprimé: Lague, D.: The stream power river incision model: evidence, theory and beyond: [Earth Surface Processes and Landforms](#), v. 39, p. 38–61, doi:10.1002/esp.3462, 2014.

Mis en forme : Anglais (E.U.)

1226 Paola, C., Straub, K., Mohrig, D., and Reinhardt, L.: The “unreasonable effectiveness” of stratigraphic
1227 and geomorphic experiments: *Earth-Science Reviews*, v. 97, p. 1–43,
1228 doi:10.1016/j.earscirev.2009.05.003, 2009.

1229 Rohais, S., Bonnet, S., and Eschard, R.: Sedimentary record of tectonic and climatic erosional
1230 perturbations in an experimental coupled catchment-fan system: *Basin Research*, v. 24, p. 198–212,
1231 doi:10.1111/j.1365-2117.2011.00520.x, 2012.

1232 Scheingross, J.S., Lamb, M.P., and Fuller, B.M.: Self-formed bedrock waterfalls: *Nature*, v. 567, p.
1233 229–233, doi:10.1038/s41586-019-0991-z, 2019.

1234 [Schwanghart, W.S., and Scherler, D.: Divide mobility controls knickpoint migration on the Roan](#)
1235 [Plateau \(Colorado, USA\): *Geology*, 48, 698-702, doi:10.1130/G47054.1, 2020.](#)

1236 Singh, A., Reinhardt, L., and Foufoula-Georgiou, E.: Landscape reorganization under changing
1237 climatic forcing: Results from an experimental landscape: *Water Resources Research*, v. 51, p. 4320–
1238 4337, doi:10.1002/2015WR017161, 2015.

1239 [Sklar, L.S., and Dietrich, W.E.: Sediment and rock strength controls on river incision into bedrock:](#)
1240 [Geology, 29, 1087-1090, 2001.](#)

1241 Sweeney, K.E., Roering, J.J., and Ellis, C.: Experimental evidence for hillslope control of landscape
1242 scale: *Science*, v. 349, p. 51–53, doi:10.1126/science.aab0017, 2015.

1243 Tofelde, S., Savi, S., Wickert, A. D., Bufe, A., and Schildgen, T. F.: Alluvial channel response to
1244 environmental perturbations: fill-terrace formation and sediment-signal disruption. *Earth Surface*
1245 *Dynamics*, v. 7, p. 609-631, doi:10.5194/esurf-7-609-2019, 2019.

1246 Turowski, J.M.: Alluvial cover controlling the width, slope and sinuosity of bedrock channels: *Earth*
1247 *Surface Dynamics*, v. 6, p. 29–48, doi:10.5194/esurf-6-29-2018, 2018.

1248 Turowski, J.M., Lague, D., Crave, A., and Hovius, N.: Experimental channel response to tectonic
1249 uplift: *Journal of Geophysical Research-Earth Surface*, v. 111, doi:10.1029/2005JF000306, 2006.

1250 [Turowski, J.M., Lague, D., and Hovius, N.: Cover effect in bedrock abrasion: A new derivation and its](#)
1251 [implication for the modeling of bedrock channel morphology: J. Geophys. Res., 112,](#)
1252 [doi:10.1029/2006JF000697, 2007.](#)

1253 [Turowski, J.M., Hovius, N., Meng-Long, H., Lague, D., and Men-Chiang, C.: Distribution of erosion](#)
1254 [across bedrock channels: Earth Surf. Process. Landforms, 33, 353-363, doi:10.1002/esp.1559, 2008.](#)

1255 Whipple, K.X., and Tucker, G.E.: Dynamics of the stream-power river incision model: Im-
1256 plications for height limits of mountain ranges, landscape response timescales, and research needs: Journal of
1257 Geophysical Research, v. 104, p. 17,661–17,674, 1999.

1258 Whittaker, A.C., and Boulton, S.J.: Tectonic and climatic controls on knickpoint retreat rates and
1259 landscape response times: Journal of Geophysical Research, v. 117, F02024, doi:10
1260 .1029/2011JF002157, 2012.

1261 Whittaker, A.C., Cowie, P.A., Attal, M., Tucker, G.E., and Roberts, G.P.: Bedrock channel adjustment
1262 to tectonic forcing: Implications for predicting river incision rates: Geology, v. 35, p. 103,
1263 doi:10.1130/G23106A.1, 2007.

1264 [Wickert, A.D., Martin, J.M., Tal, M., Kim, W., Sheets, B., and Paola, C.: River channel lateral](#)
1265 [mobilitu: Metrics, time scales, and controls: J. Geophys. Res.-Earth, 118, 396-412,](#)
1266 [doi:10.1029/2012JF002386, 2013.](#)

1267 [Zavala-Ortiz, V., Carretier, S., Regard, V., Bonnet, S., Riquelme, R., and Choy, S.: Along-stream](#)
1268 [variations in valley flank erosion rates measured using 10Be concentrations in colluvial deposits from](#)
1269 [canyons in the Atacama Desert: Geophysical Research Letters, 48, doi:10.1029/2020GL089961, 2021.](#)

Supprimé: Yanites, B.J., Ehlers, T.A., Becker, J.K., Schnellmann, M., and Heuberger, S.: High magnitude and rapid incision from river capture: Rhine River, Switzerland: Journal of Geophysical Research, v. 118, 1-25, doi:10.1002/jgrf200567, 2013.

